MODULATING FIBRIN MATRIX PROPERTIES VIA FIBRIN KNOB PEPTIDE FUNCTIONALIZED MICROGELS

A Thesis
Presented to
The Academic Faculty

by

Saranya Sathananthan

In Partial Fulfillment
of the Requirements for the Degree
Master of Science in the
School of Materials Science and Engineering

Georgia Institute of Technology
August 2012

MODULATING FIBRIN MATRIX PROPERTIES VIA FIBRIN KNOB PEPTIDE FUNCTIONALIZED MICROGELS

Approved by:

Dr. Thomas Barker, Advisor
School of Biomedical Engineering
Georgia Institute of Technology

Dr. Andrew Lyon
School of Chemistry and Biochemistry
Georgia Institute of Technology

Dr. Valeria Milam
School of Materials Science and Engineering
Georgia Institute of Technology

Date Approved: 06-26-2012

ACKNOWLEDGEMENTS

The completion of this work would not have been possible without the help of several people. First and foremost, I thank God for His faithfulness in getting me through this one day at a time. Often when I didn't think I could do it, His grace was more. God, it was your strength and power that got me through the toughest of times, even when I didn't deserve it. You provided me with the best circumstances and surrounded me with the most encouraging of people, and I am truly blessed to have had all the wonderful experiences I have had here at Tech.

I would like to thank my lab mates from both the Barker Lab and Lyon Lab for making me feel a part of the group and for assisting me in learning the different methods I needed for my project. I would especially like to thank Allyson Soon for all her help and insight into fibrin analysis techniques and assays, and Ashley Brown and Alison Douglas for helping me discuss through the possible mechanisms and quarks of my system. In the Lyon lab, I would like to especially thank Mike Smith for helping me with my conjugation strategies and Grant Hendrickson for being a good friend to talk to about not only about my project but about anything else too. I would also like to thank the Fernandez lab for helping me learn and tease through the rheology methods.

The completion of this thesis would not have been possible without the support and encouragement of my family. Even when my plans changed, you all helped me through the transition by being there for me and encouraging me to finish what I had started. Thank you for your sound guidance.

I would also like to thank Dr. Milam for being on my committee and Chris Ruffin for reminding me of the important deadlines and getting all my paper work done. Lastly, I would like to thank Dr. Barker and Dr. Lyon for really encouraging me and believing in me. Even after I decided not to pursue a PhD, you truly cared about my desires and encouraged me to pursue what would make me happy. Thank you for your persistence and for all the conversations where you lifted my spirits and confidence to be able to finish what I started here at Tech.

TABLE OF CONTENTS

LIST OF FIGURES

SUMMARY

The need to control bleeding and wound healing presents a significant clinical need in surgery, trauma, and emergency medicine. Fibrin is the body's natural provisional matrix activated in response to vascular injury, and fails in traumatic hemorrhaging due to mass dilution effects, the inability to concentrate clotting factors, and failure to generate tissue compressive forces. Noncovalent knob:hole interactions between fibrin monomers are critical for the assembly of fibrin that leads to network and clot formation. In this study we aimed to exploit fibrin knob:hole affinity interactions with swelling, space filling microgels for the development of a robust bio-synthetic hybrid polymer system with superior hemostatic properties. Previous work has explored the inherent binding interactions of various fibrin knobs and their complementary polymerization holes, which have led to the development of fibrin knob peptide mimic (GPRPFPAC) with enhanced binding affinity for fibrin(ogen) holes. By coupling this enhanced fibrinogen binding peptide with a pNIPAm microgel system capable of being dynamically tuned and self-assembled, we hypothesized the specific and rapidly triggered formation of a bulk hydrogel in a wound environment (i.e. in the presence of fibrinogen).

Additionally for fibrin-based hemostatics, there is a need to control the final macroscopic properties of the matrix to enhance cell infiltration and matrix degradation while maintaining mechanical integrity to produce hydrogels with more regenerative properties for enhanced wound healing. In this study we also sought to demonstrate the effect of fibrin knob peptide-functionalized microgels on fibrin polymerization, structure, and mechanical properties using three objectives. 1) Synthesize and characterize fibrin knob peptide-functionalized microgels 2) Characterize fibrin polymerization,

degradation, composition, and structure in the presence of fibrin knob peptide-labeled microgels 3) Determine the mechanical properties of hybrid fibrin-microgel networks. We hypothesized that fibrin polymerized in the presence of fibrin knob peptide-functionalized microgels, with specificity for fibrin(ogen) via knob:hole interactions, will result in altered polymerization dynamics, distinct fibrin polymer architectures, and altogether different physical properties of the final fibrin-microgel network.

The results of this study showed that at the microgel and peptide conjugation concentrations used, the fibrinogen triggered formation of a microgel gel did not occur. Further optimization of knob peptide-functionalized microgels should facilitate the development of a fibrinogen triggered colloidal assembly of microgels for the formation of a hydrogel for hemostatic applications. However, we did demonstrate that fibrin network polymerization, structure, and viscoelastic properties were greatly altered in the presence of knob peptide-conjugated microgels. Further investigation of hybrid microgel-fibrin systems *in vitro* will help determine the viability of these systems for different tissue engineering applications.

CHAPTER 1

INTRODUCTION

1.1 Background and Significance

The need to control bleeding and wound healing presents a significant clinical need in surgery, trauma, and emergency medicine [1]. The loss of blood remains the second most prevalent cause of death in traumatic injury, with the majority of these deaths occurring in the pre-hospital setting [1-3]. There remains a challenge for creating more robust and biocompatible hemostatic agents that are available for use by EMTs and surgeons. There are a variety of commercial hemostatics on the market such as Quick-Clot™, however this zeolite-based product known to cause exothermic burns upon use. Additionally, other hydrogel based products such as Celox™ and HemCon®, which are chitosan based products that work independently of the natural clotting process [4]. There are also thrombin and fibrin based products such as TISSEEL, Evicel®, and Crosseal™ which utilize the body's natural coagulation process to form a clot, but use high concentrations of thrombin and fibrinogen (at least an order of magnitude greater than physiological concentrations) to generate a matrix with the required mechanical stability [5]. However, at such high protein concentrations necessary to form a substantial gel, there is a significant increase in polymerization rate, and the resulting gel is comprised of highly dense fibrin networks that are not optimal for cell infiltration [6]. For fibrin based hemostatics, there is a need to control the final macroscopic properties of the matrix to enhance cell infiltration and matrix degradation while maintaining mechanical integrity to produce hydrogels with more regenerative properties for enhanced wound healing.

Fibrinogen is a 340kDa plasma glycoprotein that circulates in its inactive form in blood plasma at concentrations of 2-4mg/mL. In response to vascular injury, a fibrin polymer forms when thrombin, a serine protease, cleaves a portion of the N-termini on

the Aα-chain and Bβ-chain, known as fibrinopeptides A and B respectively. This exposes fibrin knobs ‘A’ and ‘B’ that bind to the two complementary holes ‘a’ and ‘b’ near the two distal C-termini of the γ- and Bβ-chains on a neighboring fibrin/fibrinogen monomer. These “knob: hole” interactions initiate fibrin monomer assembly in an end-to-end orientation to form fibrin protofibrils which make up the matrix network and are further stabilized by covalent crosslinking the γ- and α-chains of adjacent fibrin monomers within the protofibril [7-9].

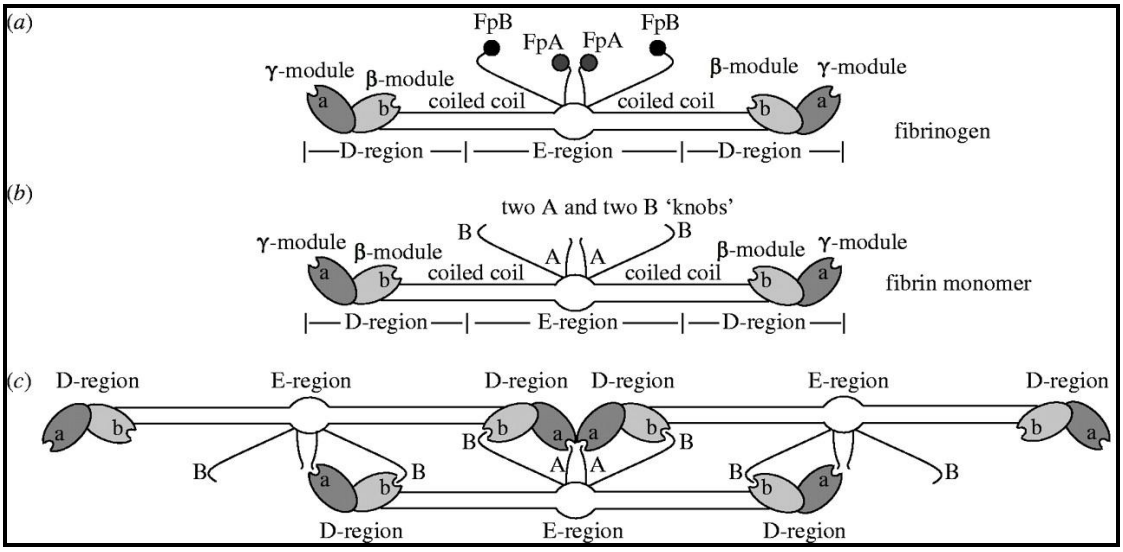

Figure 1. Fibrin Polymerization Scheme. [10]

The reason this natural hemostatic system fails in major traumatic injury is due to massive dilution, the inability to concentrate critical clotting factors, and the failure to generate tissue compressive forces during polymerization. In order for a hemostatic to facilitate the body’s natural coagulation process, it needs to be triggered by a wound environment to rapidly concentrate clotting factors, speed up the formation of a clot, and provide compressive forces on the wound during the clotting process.

This study aims to combine previous work utilizing fibrin binding mechanisms with swelling, space filling microgels for the development of a robust bio-synthetic hybrid polymer system with superior hemostatic and wound healing properties. Previous work has explored the inherent binding interactions of various fibrin knobs and their

complementary polymerization holes, which have led to the development of fibrin knob peptide mimic (GPRPFPAC) with enhanced binding affinity for fibrin(ogen) holes [11]. By coupling this enhanced fibrinogen binding peptide with a pNIPAm microgel system capable of being dynamically tuned and self-assembled, we can specifically and rapidly trigger the formation of a bulk hydrogel in a wound environment (i.e. in the presence of fibrinogen). The hypothesis is that these stimuli responsive microgels will swell and interpenetrate to form a colloidal assembly through their association with fibrinogen and provide for interesting fibrin architectures in the presence of thrombin for improved cell growth, differentiation, and remodeling for enhanced wound healing following the cessation of bleeding.

1.2 Objectives

The initial goal of this study was to determine the effect of fibrin knob peptide-functionalized ultra-low crosslinked (ULC) pNIPAm microgels as a bio-synthetic adjuvant for hemostasis. ULC microgels have the ability to swell and extensively interpenetrate to maintain microgel-microgel contacts and behave as space filling colloidal gels at high concentrations [12, 13]. We speculated that this microgel assembly could be specifically triggered by fibrinogen through active fibrin knob peptide (GPRPFPAC)-conjugated microgels with binding affinity for fibrinogen via knob:hole interactions in order to rapidly form strong, swelling, and space filling gels [11].

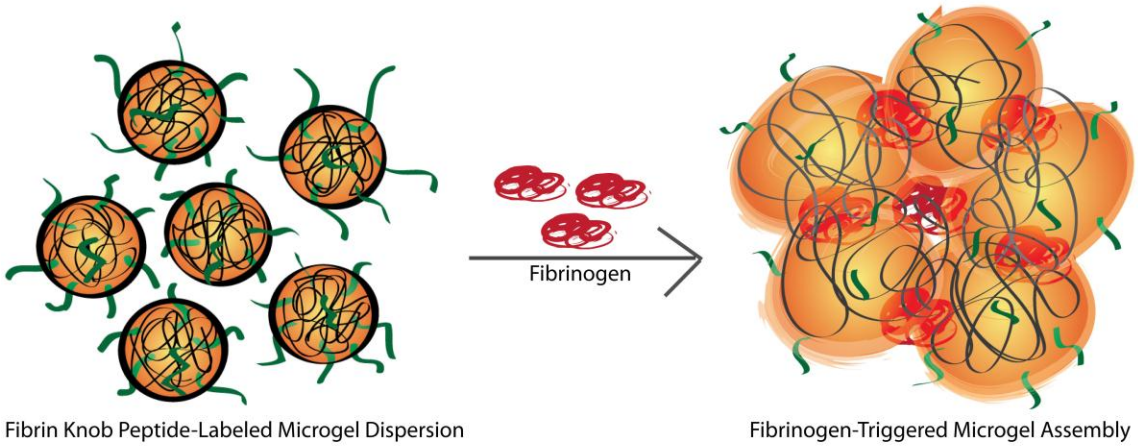

Figure 1. Schematic of Fibrinogen-Triggered Microgel Assembly

In addition, we sought to demonstrate the effect of fibrin knob peptide-functionalized microgels on fibrin polymerization, structure, and mechanical properties using three objectives. 1) Synthesize and characterize fibrin knob peptide-functionalized microgels 2) Characterize fibrin polymerization, degradation, composition, and structure in the presence of fibrin knob peptide-labeled microgels 3) Determine the mechanical properties of hybrid fibrin-microgel networks.

1.3 Hypothesis

We hypothesized that:

1) Multivalent fibrin knob peptide-labeled microgels will bind specifically to soluble fibrinogen through stable knob:hole interactions and trigger the colloidal assembly of a microgel-fibrinogen network.
2) Fibrin polymerized in the presence of fibrin knob peptide-functionalized microgels, with specificity for fibrin(ogen) via knob:hole interactions, will result in altered polymerization dynamics, distinct fibrin polymer architectures, and altogether different physical properties of the final fibrin-microgel network.

CHAPTER 2

LITERATURE REVIEW

2.1 Introduction to Fibrin Hydrogels

Fibrin networks form rapidly upon response to injury and are the body's natural provisional matrix. Fibrin based products have been optimized for a variety of different applications such as hemostatic agents, tissue sealants, and hydrogel scaffolds for tissue engineering applications [14]. As a tissue sealant, the native fibrin matrix has an advantage by promoting and stimulating cellular infiltration as a part of the wound healing process, however commercially based products have dense matrices at high protein concentrations that inhibit cell infiltration and remodeling of the matrix for proper wound healing [15]. In order to enhance the properties of a fibrin matrix, growth factors (fibroblast growth factor, endothelial growth factor, platelet derived growth factor, etc), pro-fibrinolytic proteins (plasminogen, tissue plasminogen activator), antifibrinolytic proteins (plasminogen activator inhibitor), and other extra-cellular matrix components (fibronectin, heparin) have been co-purified with plasma-derived fibrinogen in commercial products to support the formation and remodeling of the resulting matrix [16, 17]. Fibrin has been proven as a useful sealant in cardiac, liver, and spleen surgery, and fibrin hydrogels have been used widely in the recent decade in a variety of tissue engineering applications such as the tissue engineering of adipose, cardiovascular, ocular, muscle, liver, skin, cartilage, and bone tissues [14].

2.2 Biosynthetic Fibrin-Polymer Hydrogels

Fibrin hydrogels comprised of physiological levels of protein have three major disadvantages as a scaffold in regenerative medicine: the shrinkage of the gel during the formation of flat sheets, low mechanical stiffness, and rapid degradation before the

proper regeneration of tissue [14, 18, 19]. In order to improve these properties and increase the mechanical stiffness and stability of the matrix, fibrin hydrogels have been combined with numerous other scaffold materials including polyurethane [20], polyethylene oxide [21], polycaprolactone [22], heparin [23], collagen [24], hyaluronic acid [25], poly(L-lactic acid) and polylactic-glycolic acid [26], and polyethylene glycol (PEG) [27].

Fibrin-based PEG hybrid scaffolds have been extensively studied in order to combine the favorable mechanical properties of PEG with the biological properties of fibrin. By denaturing fibrinogen and reducing disulfide bonds, then re-crosslinking the free sulfhydryl's using PEG-diacrylate, Dror Seliktar's group has utilized a multitude of PEG-fibrin gels with tunable structural characteristics that exhibited a range of elastic moduli, degradation rates, and cellular invasion kinetics [28-30]. Other groups have utilized fibrin based peptide-modified PEG in order to alter fibrin polymerization characteristics and physical properties of the formed hydrogel [5, 15, 31, 32].

Other groups have co-polymerized fibrin with other hydrogels. Akpalo et al., have created interpenetrating networks of polyethylene oxide and fibrin polymerized in juxtaposition to greatly enhance the mechanical properties of a fibrin gel and permit cell growth [21]. Lesman et al, showed the combination of PLLA/PLGA sponges embedded with a fibrin matrix provided added mechanical strength to the construct and featured highly mature vessel-like networks *in vitro* and *in vivo* [26]. Dare et al., demonstrated that a genipin crosslinked fibrin hydrogel did not significantly affect cell viability, but greatly increased the dynamic compression and shear modulus of the hydrogel for improved mechanical properties [33]. These studies show the potential of combining the mechanical properties of a polymer with the biological properties of fibrin in order to construct scaffolds with enhanced regenerative potential.

2.3 Modifying Fibrin Matrices through Fibrin Knob Mimicking Peptides

The polymerization of fibrin involves the noncovalent association of four types of knob:hole interactions on fibrin molecules: A:a, A:b, B:a, and B:b. The evidence for these knob:hole interactions was first shown when fibrin polymerization was inhibited by synthetic knob 'A' tripeptides GPR (Gly-Pro-Arg) competing for fibrin holes [34, 35]. Characterization of the equilibrium binding affinities of knob 'A' and 'B' variants to fibrinogen showed that knob 'A' peptide mimics GPRV and GPRP have higher affinities to fibrinogen than knob 'B' GHRP and AHRP mimics under calcium-free conditions [34-36]. By investigating the binding events of these mimics under dynamic conditions using surface plasmon resonance (SPR), the residence time of noncovalent knob:hole interactions was determined to further understand fibrin assembly initiation and polymerization [11]. In this study, a novel knob 'A' mimic (GPRPFPAC) was presented that has a 10-fold higher association rate (12.5×10^{-3} $M^{-1}s^{-1}$) than current mimics.

Using fibrin knob peptide technology, several methods for altering fibrin network structure have been employed. Knob peptide-protein constructs using GPRP, GPRV, GHRP, and GSPE conjugated to the integrin-binding fibronectin 9^{th} and 10^{th} type III repeats (FnIII9-10) were shown to bind stably to fibrin(ogen) via specific knob:hole interactions and were retained within fibrin matrices under excessive perfusion [37]. Fibrin matrix properties were also altered using bivalent and tetravalent knob peptide-PEG conjugates and revealed that although a significant change in network structure was observed, clotting time and degradation rates were not significantly altered [32]. Fibrin assembly was also inhibited using PEGylated fibrin knob mimics, where a 10-fold enhancement of anticoagulant activity was observed with active peptides PEGylated with 5 kDa PEG [5]. Additionally in order to determine the interaction of peptides specific for hole 'b', the knob peptide (AHRPYAAC)-PEG conjugate was showed to enhance the porosity and diffusivity of a fibrin matrix while also increasing the viscoelastic properties and decreasing the susceptibility to degradation [15]. These studies have all shown

potential knob peptide-conjugate designs that alter fibrin polymerization and structure for a variety of different applications.

2.4 pNIPAm Microgels in Biomedical Applications

Synthetic hydrogels are gels that swell strongly in aqueous media and are typically composed of a hydrophilic organic polymer component that is cross-linked into a network by either covalent or noncovalent interactions [38-40]. By using specific chemistries and designs, hydrogels have become paramount in areas such as in vivo diagnostics, drug and gene delivery, chemical separations, chemical and biological sensors, and optical materials [41]. Stimuli-sensitive hydrogels that change in swelling due to subtle environmental changes are of particular interest, and one specific stimuli-sensitive polymer with emerging potential in biotechnological applications is poly(*N*-isopropylacrylamide) (pNIPAm). pNIPAm is a thermoresponsive hydrogel, characterized by a sharp volume phase transition at a lower critical solution temperature (LCST) where hydrogen bonds with the polymer chain are broken, entropically driving the formation of a globular polymer conformation [41]. Thus, at temperatures higher than the volume phase transition temperature (VPTT), the hydrogel goes from a swollen, hydrophilic state to a compact, relatively hydrophobic state. pNIPAm hydrogels have been synthesized by a variety of different techniques and various functional groups have been added to the polymer by copolymerization ad post-polymerization modifications [42].

pNIPAm microgels have similar properties as their bulk counterpart, and also undergo a VPPT near the LCST of the polymer [43, 44]. Microgels are colloidally stable hydrogels whose size can vary from tens of nanometers to micrometers [45, 46] and posses unique characteristics for different applications due to their colloidal properties. pNIPAm microgels are synthesized by free-radical precipitation polymerization whereby a NIPAm solution containing an initiator and cross-linker is heated to above the LCST of the polymer (70°C) causing the free radical initiator to attack NIPAm monomers causing

radical propagation and chain growth. Once the chain reaches a critical length, it collapses on itself producing precursor particles that grow by aggregation with other precursor particles and upon cooling result in the formation of stable microgels.

Usually the presence of a cross-linker is critical in preventing the dissolution of the polymer particle once it is cooled below the LCST, however, Gao and Frisken have shown that it is possible to make pNIPAm microgels by precipitation polymerization without using a cross-linker [47, 48]. These ultra-low crosslinked (ULC) microgels are "self-crosslinked" by a chain transfer reaction occurring at either or both of two possible sites: the hydrogen atom attached to the tertiary carbon atom on the pendant isopropyl group and the hydrogen atom on the tertiary carbon atom of the main-chain backbone. Additionally, these ULC microgels are characterized by low solid content and larger swelling ratios as compared to N,N-methylene bis(acrylamide) (BIS) crosslinked microgels [47, 48]. Another interesting property of ULC microgels is their ability to swell and self-associate as space filling colloidal gels in order to maximize their local coordination number [12, 13].

A variety of different pNIPAm and poly(N-isopropylmethacrylamide) (pNIPMAm) based microgels have been biofunctionalized for a variety of different applications including targeted gene delivery [49], thermally modulating enzyme activity [50], and DNA detection [51] amongst others. Thus pNIPAm ULC microgels present a viable option for bioconjugation with fibrin knob peptides, and present unique colloidal properties for interaction with fibrinogen and altering fibrin matrix properties.

2.5 Conclusion

By biofunctionalizing ULC microgels with fibrin knob peptides the hope is to dynamically trigger the colloidal assembly of microgels through knob:hole interactions in the presence of fibrinogen. How these peptide-functionalized microgels alter fibrin

polymerization, network structure, and physical properties are important factors determining cell fate for precise wound healing.

CHAPTER 3

FIBRIN KNOB PEPTIDE FUNCTIONALIZED PNIPAM MICROGEL SYNTHESIS AND CHARACTERIZATION

3.1 Introduction

Previously, bivalent and tetravalent knob peptide-PEG conjugates have shown to alter fibrin polymerization kinetics and structure by actively engaging alternative polymerization mechanisms through knob:hole interactions [32]. The goal of this study was to utilize multivalent knob peptide-fibrinogen interactions to rapidly form a network even in the absence of clotting enzymes. In order to create a gel network triggered by the presence of fibrinogen, we rationally designed fibrin knob peptide (GPRPFPAC) displaying ultra-low crosslinked microgels that would associate with one another through fibrin knob:hole interactions and swell and interpenetrate to form a colloidal assembly.

We developed a synthesis and conjugation strategy for active knob peptide (GPRPPFAC) and non-binding control peptide (GPSPFPAC)-displaying microgels. First, ultra-low crosslinked (ULC) pNIPAm microgels were copolymerized with 5% acrylic acid (AAc) using standard precipitation polymerization techniques to allow for further functionalization of the acid groups with fibrin knob peptides. A heterobifunctional linker, N-ε-maleimidocaproic acid hydrazide, trifluoroacetic acid salt (EMCH), was then conjugated to the carboxyl functional groups on the microgel for subsequent maleimide coupling to cysteine terminated fibrin knob peptides.

Unfunctionalized ULC microgels were characterized using dynamic light scattering to determine hydrodynamic radius and particle polydispersity. The peptide-microgel bioconjugation reaction was monitored using Ellman's assay for free sulfhydryls to ensure complete peptide conjugation. Peptides conjugated to the microgel were then quantitated using a CBQCA protein quantitation assay. A modified ELISA was

performed to determine basic binding affinity of fibrinogen for active fibrin knob peptide (GPRPFPAC)-microgels.

3.2 Methods

3.2.1 Materials

All chemicals used during microgel synthesis (N-isopropylacrylamide, acrylic acid, and ammonium persulfate) were purchased from Sigma-Aldrich (St. Louis, MO) and used as received unless otherwise noted. The monomer N-isopropylacrylamide (NIPAm) was recrystallized from hexane (J.T. Baker) before use. Water used during the synthesis, purification, and characterization of microgels was distilled and then deionized using a Barnstead E-pure system operating at a resistance of 18MΩ. GPRPFPAC and GPSPFPAC peptides were ordered from GenScript Corp (Piscataway, NJ). The chemicals used for making conjugation and assay buffers were HEPES (EMD Chemicals, Cincinnati, OH), MES (EMD), sodium chloride (NaCl) (Fisher Scientific, Pittsburgh, PA), calcium chloride ($CaCl_2$) (Fisher Scientific), formic acid (VWR, Radnor, PA), EDTA (Lonza, Allendale, NJ), BSA (EMD), Tween 20 Polysorbate 20 (VWR), DMSO (Amresco, Solon, OH), sodium borate (J.T. Baker), and sulfuric acid (H_2SO_4) (VWR). The coupling reagents used for peptide conjugation to microgels were N-ε-maleimidocaproic acid hydrazide, trifluoroacetic acid salt (EMCH) (Thermo Scientific, Rockford, IL), 1-ethyl-3methyl-(3-dimethylaminopropyl) carbodiimide (EDC) (Thermoscientific), and N-hydroxysulfosuccinmide (NHSS) (Thermoscientific). For Ellman's assay the chemicals needed were Ellman's reagent 5,5'-Dithio-bis-(2-nitrobenzoic acid) (DTNB) (Thermoscientific) and L-(+)-Cysteine Hydrochloride Monohydrate (J.T. Baker). The CBQCA protein quantitation kit was purchased from Invitrogen (Frederick, Maryland) for peptide quantitation. The reagents used in the ELISA binding assay were polyethyleneimine (PEI) (J.T. Baker), N-Hydroxysuccinimide

(NHS) (Thermoscientific), human fibrinogen (FIB-3, Enzyme Research Laboratories, South Bend, IN), HRP-conjugated goat anti-fibrinogen antibody (MP Biomedicals #55239), and 1-step Ultra TMB substrate (Pierce #34028).

3.2.2 Ultra-Low Crosslinked (ULC) pNIPAm Microgel Synthesis

Ultra-low crosslinked pNIPAm microgel particles were synthesized by free-radical precipitation polymerization. The molar composition used was 95% N-isopropylacrylamide (NIPAm) and 5% acrylic acid (AAc), with a total monomer concentration of 140 mM. Copolymerization with AAc was done to allow for chemoligation sites for peptide attachment. Reaction conditions were used that favor chain transfer reactions at the polymer backbone which lead to cross-linking between chains without the need for additional cross-linking monomers [47, 48]. In a typical reaction, 100 mL of a filtered aqueous solution of recrystallized NIPAm and AAc was added to a reaction flask and heated to 70°C at a temperature ramp of 60°C/hr. The solution was purged with N_2 gas and stirred at 450 rpm while heating until the temperature remained stable. In order to initiate the polymerization reaction, a filtered 1 mL solution of ammonium persulfate (APS) was added to make the final concentration of APS in the reaction ~1 mM. The solution turned turbid, indicating successful initiation. The reaction was allowed to continue at 70°C for 5 hours under a N_2 blanket and continuous stirring before allowing the solution to cool to room temperature. Following synthesis, the solution was filtered through glass wool to remove a small amount of coagulation, and purified 5X by centrifugation at 100,000 rpm for 15 minutes and resuspension in dH_2O. The microgels were lyophilized until further use.

3.2.3 Dynamic Light Scattering (DLS) Particle Analysis

Monodispersity and hydrodynamic radius of the microgels were determined using dynamic light scattering (DLS) at 25°C in pH 3 0.1 M formate buffer. A dilute microgel

solution in formate buffer was allowed to equilibrate for 10 minutes prior to taking 5 measurements of 20 readings each to obtain an average value for the hydrodynamic radius and polydispersity.

3.2.4 Fibrin Knob Peptide Conjugation to Microgels

Fibrin knob peptides with sulfhydryl-containing cysteine-terminated ends (GPRPFPAC and the non-binding control peptide GPSPFPAC) were the two peptides used for conjugation to microgels. Peptide conjugation to pNIPAm microgels was done using a two-step conjugation method. Firstly, a maleimide-functionalized microgel was produced through EDC/NHSS coupling of a heterobifunctional crosslinker, N-ε-maleimidocaproic acid hydrazide, trifluoroacetic acid salt (EMCH) to the carboxyl groups on the microgel. Then the fibrin knob peptides were conjugated to the EMCH groups on the microgels via maleimide coupling to the free cysteine residues on the C-termini of the peptides. Peptide coupling was done by introducing the peptides at a 1:1 molar ratio with the carboxyl groups. Coupling reagents were used in 10 mol excess of peptide to ensure complete coupling and all bioconjugation reactions were carried out in a 10 mL reaction volume.

For the first step of the coupling process, the calculated amount of microgels was resuspended at room temperature in pH 5.0 MES buffer overnight. 1-ethyl-3methyl-(3-dimethylaminopropyl) carbodiimide (EDC) and N-hydroxysulfosuccinmide (NHSS) were reacted with the microgel solution for 30 minutes on a shaker to activate the carboxyl groups. The EMCH was then added to the microgel solution and reacted for 2.5 hours to permit coupling between the carboxyl reactive hydrazide groups on the EMCH and the carboxyl groups on the microgel surface. In order to remove any unreacted material and to exchange to a pH 7.4 25 mM HEPES, 25 mM NaCl buffer for the maleimide coupling, a 10 kDa snake skin dialysis membrane (Thermoscientific, Rockford, IL) was used and the buffer replaced 5 times every 4 hours. For the second step of the conjugation reaction,

the appropriate amount of peptide was added to the maleimide activated microgels and reacted overnight on a shaker. Excess unconjugated peptide was removed from the peptide-functionalized microgels using the 10 kDa snake skin membrane and dialyzed into dH_2O with the solution being replaced 5 times every 4 hours. The resulting product was aliquoted, lyophilized and quantified.

3.2.5 Ellman's Assay for Free Sulfydryls

The bioconjugation reaction was monitored using Ellman's assay for free sulfhydryls. 5,5'-dithio-bis-(2-nitrobenzoic acid), also known as DTNB or Ellman's Reagent, is a water-soluble compound used for quantitating free sulfhydryl groups in solution [52]. DTNB reacts readily with a free sulfhydryl group to yield a mixed disulfide and 2-nitro-5-thiobenzoic acid [52], which produces a yellow-colored product which can be measured using a standard plate reader. This reagent can be used to detect the free sulfhydryl groups on C-terminal cysteines and determine the concentration in solution by comparison to a standard curve of known concentrations of a sulfydryl-containing compound.

Ellman's assay was used to determine if there were any unreacted peptides in the bioconjugation reaction of the fibrin knob peptides with the maleimide functionalized microgels. The detectable range of the assay is 0.1 – 1.0 mM, and the standard curve was generated using cysteine standards. Free peptide, unconjugated microgels, and (unconjugated microgels + free peptide) were used as controls. The conjugation reaction was monitored for 1hour to detect for the presence of unconjugated peptide.

In order to prepare the Ellman's reagent, 4.5 mg of DTNB was dissolved into 3 mL of a pH 7.4 25 mM HEPES, 25 mM NaCl, 1 mM EDTA reaction buffer. 5 uL of this Ellman's solution and 85 uL of the reaction buffer were added to each well of a 96 well plate. 10 uL of each sample was added to separate wells at time points of 0, 15, 30, 45,

and 60 mins, and the absorbance of the solution was measured at 412 nm using a SpectraMax M2 Microplate Reader (Molecular Devices, Sunnyvale, CA).

3.2.6 Peptide Quantitation Assay

Amines on the peptide-labeled microgels were quantified using the CBQCA Protein Quanititation Kit with the respective peptides used to generate the standard curve. The CBQCA protein quantitation assay is a quick and highly sensitive method for the quantitation of proteins in solution ranging from 10 ng-150 ug of protein [53]. The ATTO-TAG™ CBQCA reagent is used to quantitate primary amines in solution, including the accessible amines in proteins and peptides, by forming highly fluorescent derivatives in the presence of cyanide that can be measured using a standard plate reader. [53].

Peptide standards and peptide-microgel samples were prepared in pH 9.3 0.1 M sodium borate buffer for a final volume of 135 uL added to separate wells of a 96 well plate. 5 uL of a 20 mM potassium cyanide (KCN) solution was added to each well. A 5 mM working solution was prepared from a 40 mM CBQCA stock solution, and 10 uL of this working solution was added to each well, mixed on an Eppendorf MixMate at 400 rpm and allowed to incubate for 1 hr in the dark before measuring the fluorescence at Ex. 465 nm/Em. 550 nm using a BioTek Synergy H4 Hybrid Multi-Mode Microplate Reader (BioTek, Winooski, VT).

3.2.7 Fibrinogen-Microgel Binding Affinity Assays

A modified ELISA technique was used to determine the affinity of fibrinogen for the various fibrin knob peptide-labeled microgels covalently immobilized to the bottom of 96 well plates via their carboxyl containing groups using EDC/NHS chemistry. 5 mg/mL polyethyleneimine (PEI) was used to coat Corning® clear bottom 96 well plates (Sigma Aldrich) for at least 2 hours in order to create a positively charged hydrophilic

surface. After washing the plates, 1 mg/mL microgel solutions in dH_2O were centrifugally deposited for 10 min at 3700 rpm, then conjugated directly to the PEI layer via additional unreacted carboxyl groups on the peptide-labeled microgels using EDC/NHS. Unreacted microgels were removed by washing with dH_2O, and were blocked with HEPES + Ca + 1% BSA buffer (25 mM HEPES, 150 mM NaCl, 5 mM$CaCl_2$, pH 7.4) for 1 hour prior to the fibrinogen binding step.

Human fibrinogen at 25 ug/mL was incubated with the microgel substrates and unbound protein removed by washing. Bound fibrinogen was detected using HRP-conjugated goat anti-fibrinogen antibody and 1-step Ultra TMB substrate. The detection antibody was added at a concentration of 1:50,000 in 1% BSA to each well and incubated for 1hr before washing off any unbound antibody. TMB substrate was added to each well and allowed to incubate for 8min at room temperature. The TMB reaction was quenched with 1 M H_2SO_4 before measuring the Absorbance at 450 nm using a BioTek Synergy H4 Hybrid Multi-Mode Microplate Reader (BioTek, Winooski, VT). All intervening wash steps were conducted using HEPES + Ca + 0.05%Tween-20 buffer; and all binding steps were conducted using HEPES +Ca +1% BSA buffer. A standard curve was generated using dilutions of fibrinogen bound directly to the plate, and each condition was tested with at least 9 samples.

3.3 Results

3.3.1 Hydrodynamic Radius of Microgels

The hydrodynamic radius $\langle R_h \rangle$ of 5% AAc-pNIPAm microgels at 25°C in pH 3 0.1 M formate buffer as measured by DLS was 474.1 nm, with a polydispersity index of 0.07 indicating that the microgels are roughly 1 um in diameter with relative monodispersity.

3.3.2 Monitoring the Peptide Conjugation Reaction

The microgel concentration in the GPRPFPAC-microgel bioconjugation reaction was estimated to be 1.28 mg/mL, and the peptide concentration in the reaction was estimated to be 0.567 mM. To reflect similar concentrations, the unconjugated microgel control was measured at 1.28 mg/mL, and the GPRPFPAC free peptide control was measured at 0.5 mM. The microgel concentration in the GPSPFPAC-microgel bioconjugation reaction was estimated to be 1.715 mg/mL, and the peptide concentration in the reaction was estimated to be 0.757 mM. To reflect similar concentrations, the unconjugated microgel control was measured at 1.715 mg/mL, and the GPSPFPAC free peptide control was measured at 0.75 mM. Based on the cysteine standard curve, the controls fall within the correct concentration range (Fig. 3). The results of the assay demonstrate that the peptides react with the maleimide functionalized microgels almost instantaneously after being added to solution, but do not react with unconjugated microgels, indicating that the bioconjugation reaction is a specific and rapid reaction carried out to completion in approximately one hour. The peptide-microgel conjugation reaction was allowed to carry out for at least 2.5 hours to ensure complete conjugation.

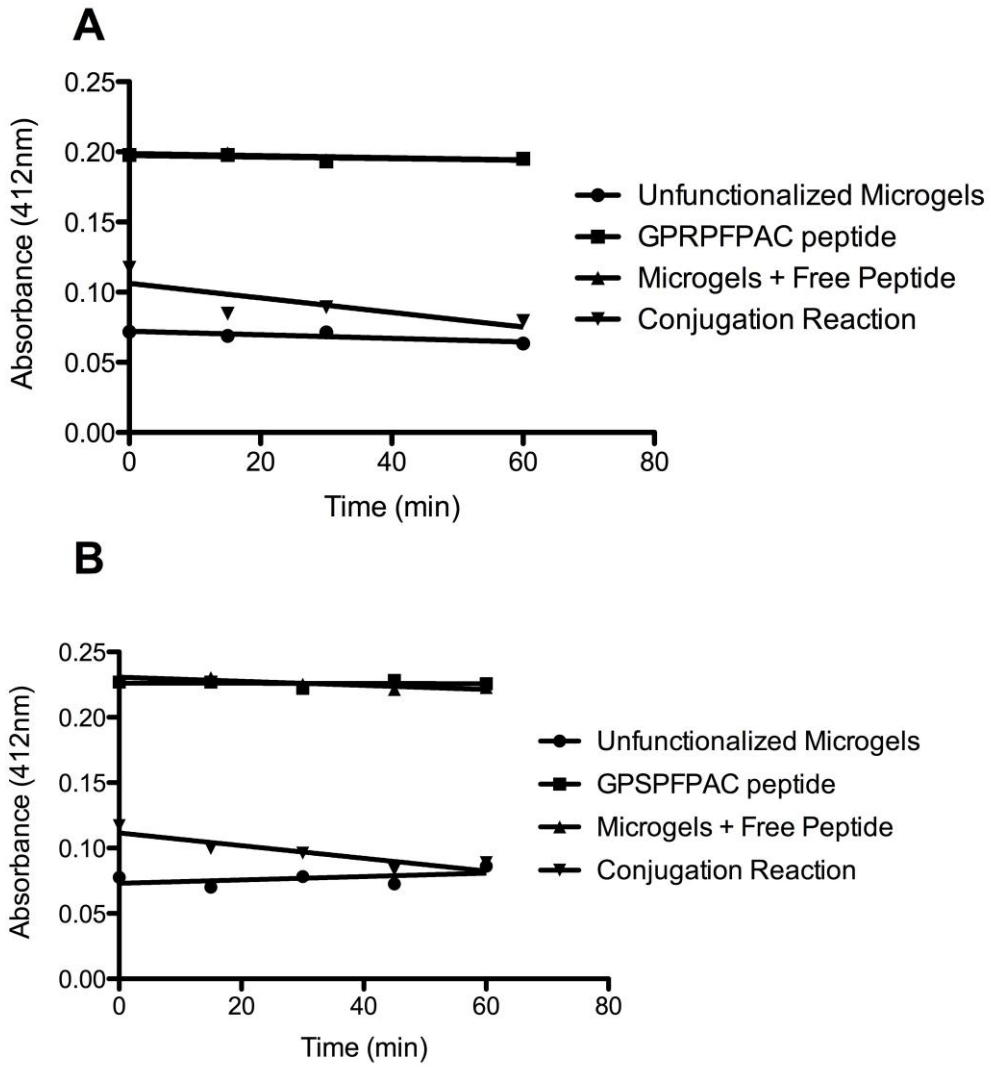

Figure 3. Ellman's Assay for Monitoring Peptide Conjugation to Microgels. (A) GPRPFPAC-microgel bioconjugation reaction, showing reaction specificity of peptides for EMCH conjugated microgels (B) GPSPFPAC-microgel bioconjugation reaction, showing similar reaction time and specificity for EMCH conjugated microgels.

3.3.3 Peptide Quantification

The CBQCA protein quantitation assay was used to quantify amines on fibrin knob peptide labeled microgels in order to determine the amount of peptide conjugated per milligram of microgels. A standard curve was generated using triplicate samples of peptide solutions ranging from 0 mM to 0.75 mM. Linear regression analysis was performed for each peptide standard, which resulted in a line of best-fit for GPRPFPAC;

y=36730x + 3959 with an r^2 value of 0.938, and GPSPFPAC; y=25800x + 2128 with an r^2 value of 0.9604. An estimate of the amount of peptide per milligram of microgels was determined from these peptide standard curves. The amount of GPRPFPAC peptide per miligram of microgels is 1.45e-8 mols , which corresponds to a peptide concentration of 0.0145 mM per mg/mL of microgels. The amount of GPSPFPAC peptide conjugated to a miligram of microgels is 8.1e-8 mols, which corresponds to a peptide concentration of 0.081 mM per mg/mL of microgels.

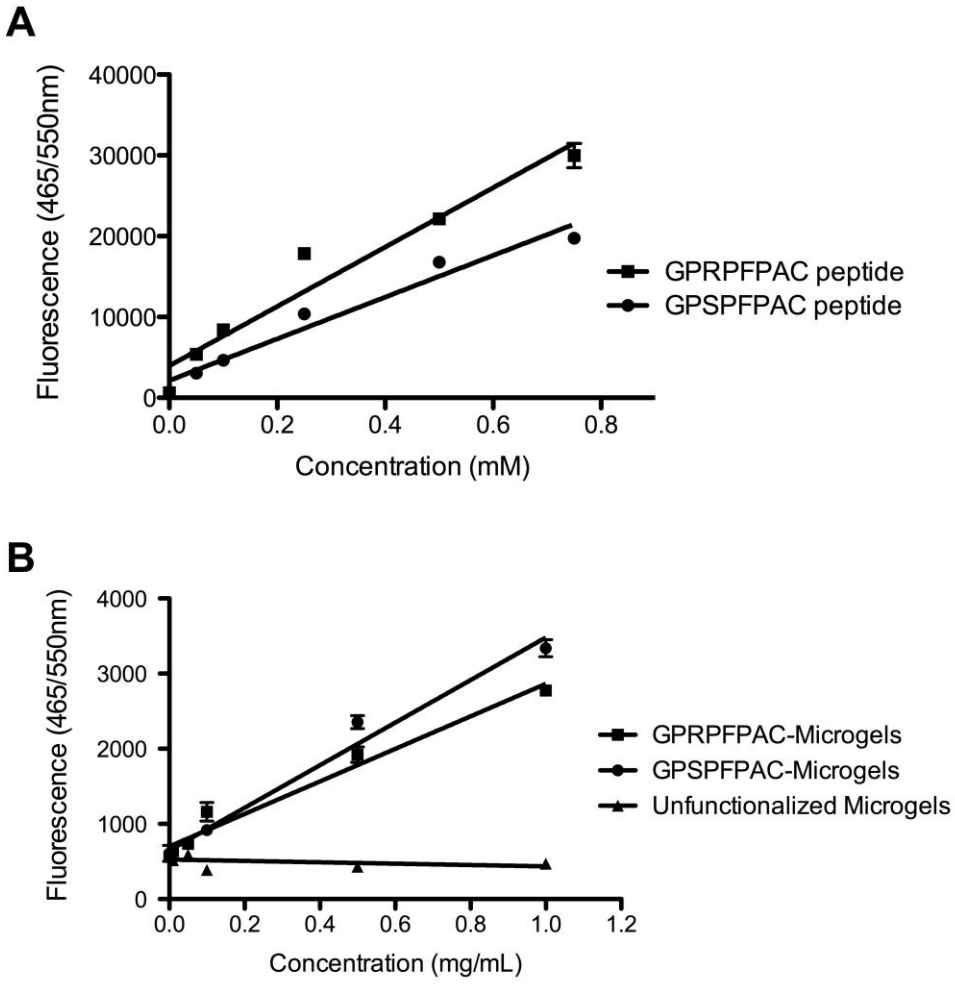

Figure 4. CBQCA Peptide Quantitation Assay of Peptide Functionalized Microgels. (A) Standard curve of respective fibrin knob peptides (B) peptide quantitation of peptide-microgels showing microgel concentration dependent signal.

3.3.4 Fibrinogen Binding Affinity for Peptide Modified Microgels

In order to determine the basic binding affinity of fibrinogen for GPRPFPAC-microgels, a modified ELISA technique was used to detect fibrinogen bound to microgel coated plates by using an anti-fibrinogen HRP-conjugate. The amount of soluble fibrinogen absorbed to the microgels was normalized against the signals obtained from dilutions of fibrinogen bound directly to the plate. The ELISA results indicate that soluble fibrinogen preferentially bound to GPRPFAC-microgel coated wells, but not the unfunctionalized microgels or the non-binding GPSPFPAC-microgel controls. An unpaired t-test with a 95% confidence level and corresponding p value <0.05 was considered significant (Prism 5, GraphPad Software, Inc., La Jolla, CA).

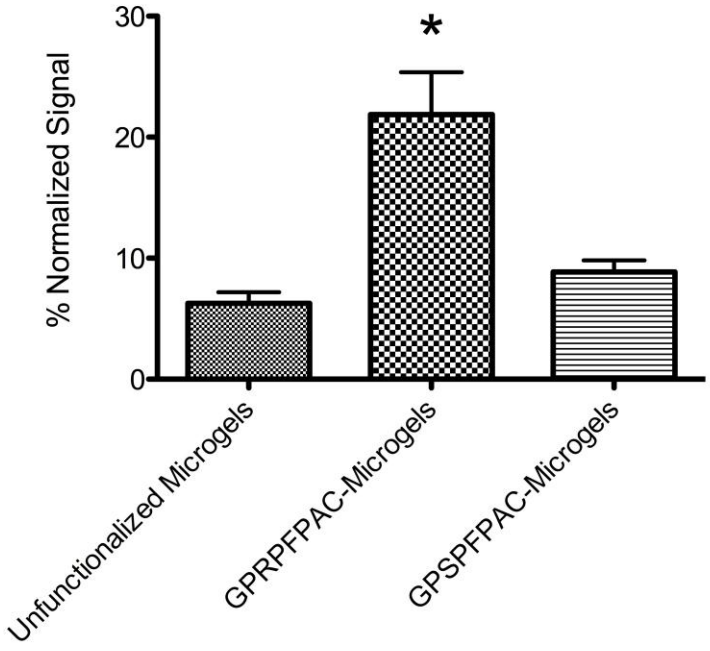

Figure 5. ELISA studies analyzing fibrinogen affinity for GPRPFPAC-microgels. Fibrinogen affinity for GPRPFPAC-microgels as compared to unfunctionalized microgels and non-binding GPSPFPAC-microgel control. The amount of soluble fibrinogen absorbed to the microgels was normalized against the signals obtained from dilutions of fibrinogen bound directly to the plate.* denotes $p<0.05$ relative to all groups.

3.4 Discussion

The CBQCA peptide quantitation assay is a simple estimate for the amount of peptide conjugated to the microgels. The results showed that even though sufficient numbers of peptide were conjugated to the microgels, based on the amount of peptides conjugated per mg of microgel and the amount of microgels used for conjugation, the calculated percent yield for peptide conjugation to the microgels was extremely low. The percent yield for GPRPFPAC peptide conjugation to the microgels was only 3.3% and slightly higher for GPSPFPAC peptide conjugation at 18.3%. Although the ELISA results show preferential binding of fibrinogen to the active knob peptide (GPRPFPAC)-microgels, the amount of fibrinogen bound to the microgels is only slightly over 20% of 25 ug/mL fibrinogen bound directly to the bottom of an unblocked plate. These results show that while the formation of multivalent peptide-displaying microgels with specificity for fibrinogen is possible, better control of the conjugation reaction, more efficient binding of peptides to the microgels, and better control of ligand density is required for homogeneous multivalent display of peptides on the microgel.

Although the Ellman's assay results suggest complete conjugation of the peptides to the microgels, it is possible that the loss in signal is due to peptide dimer formation that occurs through disulfide bonds via the free C-termini cysteines on the peptides. In order to prevent the formation of dimers, the reaction pH and reducing/oxidizing conditions need to be monitored closely and the conjugation reaction possibly altered completely to facilitate more efficient peptide conjugation.

Peptide ligand density and homogenous or heterogeneous display of peptides on the microgels is a critical factor influencing peptide-fibrinogen association to form a colloidal assembly and a key parameter influencing fibrin polymerization. Multi-angle laser light scattering of ULC microgels can be used to determine the molecular weight of the microgels and allow for the estimate of the number of peptides conjugated per microgel. While this was not performed with the microgels in this study, because the

percent yield of peptides conjugated to the microgels is so low, it suggests the formation of heterogeneous peptide display on the microgels. Better control of ligand density on the microgels is necessary for further study of fibrin knob peptide-microgel interactions with fibrin(ogen). Studying the influence of ligand density on microgel assembly formation and fibrin polymerization is crucial for determining optimal peptide multivalency for triggering a colloidal assembly of microgels and significantly altering fibrin polymerization. The rational design of the next generation of peptide-microgel conjugates will be described in the discussion of the next chapter.

CHAPTER 4

HYBRID MICROGEL-FIBRIN CLOTS: ALTERING FIBRIN POLYMERIZATION, COMPOSITION, AND STRUCTURE

4.1 Introduction

By synthesizing multivalent fibrin knob peptide-conjugated microgels, we hoped to trigger the colloidal assembly of microgels through knob:hole interactions in the presence of fibrinogen. We measured fibrinogen-microgel assembly by observing the change in turbidity upon the addition of fibrinogen to a solution of peptide-conjugated microgels and physically determined whether a gel was formed. However, the peptide-microgel concentration was not optimal for forming a colloidal assembly in the presence of fibrinogen alone.

Despite this, we predicted that in the presence of low concentrations of thrombin, knob peptide-conjugated microgels would act as an adjuvant for fiber network formation and increase the overall rate of polymerization into a gel network by providing nucleation sites through multivalent peptide display for association with fibrin monomers for the formation of a microgel-fiber network.

The dynamics of fibrin assembly into a network and alterations to assembly kinetics have been extensively studied [54]. Fibrin network polymerization kinetics and structure can be modified by varying ionic strength (NaCl concentration), calcium concentration, fibrinogen and thrombin concentration, pH, and the use of alternative thrombin-like clotting enzymes [55-57]. Knob:hole interactions initiated by the removal of fibrinopeptides are crucial in determining important network parameters such as fiber diameter and branching, both of which can be detected from clot turbidity measurements [58]. Translucent clots are formed with high thrombin concentrations or high NaCl concentrations, and are commonly interpreted to be thin, highly-branched networks.

Opaque clots are formed at low NaCl or high calcium concentrations, which are conditions that have been shown to favor lateral aggregation of the fibrin protofibrils, giving rise to thicker bundles that scatter more light.

The addition of synthetic fibrin knob peptide mimics alters fibrin matrix formation and perturbs clot turbidity depending on the type of knob mimic [35]. At high concentrations over 100-fold molar excess, fibrin knob 'A' peptide derivatives such as GPRP-mimics inhibit fibrin polymerization and increase fibrinogen clotting time by competing with native fibrin knobs for polymerization hole domains [34]. However, at a 1:1 molar ratio, fibrin polymerization is not inhibited but rather fibrinogen molecules are pre-engaged through knob:hole interactions with the peptides prior to fibrin polymerization [15].

In addition to the alteration of fibrin polymerization and structure through the addition of fibrin knob peptide mimics, bivalent and tetravalent knob-PEG conjugates with size ranges from 2 to 20 kDa have shown to alter the clotting characteristics of fibrin in a dose-dependent manner, with conjugate size playing a major role in changing fibrin network structure [32]. PEGylated fibrin knob 'A' peptides demonstrated a biphasic effect of PEG chain length, with increasingly enhanced inhibition of fibrin polymerization from 0 to 5 kDa, but above 5 kDa returning to control levels [5]. Other polymers, either natural or synthetic, have been copolymerized with fibrin, embedded within fibrin matrices, or cross-linked with fibrin in order to combine the properties of the two polymers for enhanced mechanical strength, greater resistance to degradation, increased protein retention, and unique architectures for various tissue regeneration applications.

In vivo, the events that trigger coagulation also initiate the process of fibrinolysis through the activation of plasminogen to generate the active serine protease, plasmin. The fibrinolytic process is modulated by a complex of several biochemical processes involving plasminogen activators, plasminogen activator inhibitors, and fibrinolysis

inhibitors. Exogeneous fibrinolysis, which is independent of plasmin activation, involves overlaying a solution of active plasmin on top of a stable clot and measuring the surface degradation [59]. Exogeneous fibrinolysis is a diffusion dependent phenomenon and the lysis rate has been shown to decrease with fibrin fiber diameter [59-61]. Another study showed that thinner fibers are digested more quickly, but thicker fibers are more likely to undergo agglomeration, which has been shown to accelerate fibrinolysis [62]. The introduction of fibrin knob peptide-PEG conjugates to a fibrin polymer resulted in more porous networks with nearly doubled effective diffusion coefficients over control groups, however, because the degradation profiles were similar, it was speculated that lysis is mediated both by diffusion limits and conformational alterations in the fibrin fibers [15]. Diffusion into fibrin knob peptide-PEG conjugate fibrin gels occurred at a faster rate due to the coarsely porous network, but plasmin binding and lysis occurred at a slower rate due to the structural alteration of fibrin fibers [15].

We hypothesize that fibrin polymerized in the presence of fibrin knob peptide-functionalized microgels will alter polymerization kinetics, degradation rate, protein composition and fibrin network structure. Microgel size and concentration, peptide ligand density, and thrombin concentration are expected add to the complexity of this fibrin-microgel system. We studied the polymerization kinetics of fibrin polymerized in the presence of various peptide-microgel conjugates through clot turbidity measurements, analyzed the soluble protein in the final clot using a Quant-iT™ Protein Assay, analyzed the degradation rate by an exogenous fibrinolysis assay, and observed the structure of the resulting network by confocal microscopy.

4.2 Methods

4.2.1 Materials

Synthesized unfunctionalized pNIPAm microgels, GPRPFPAC-microgels, and GPSPFPAC-microgels, all described in Chapter 3, were used for these studies. Human fibrinogen FIB-3 and human α-thrombin were purchased from Enzyme Research Laboratories (South Bend, IN). For the buffers HEPES (EMD), NaCl (Fisher Scientific), $CaCl_2$ (Fisher Scientific), and deionized and distilled water were used. Alexa Fluor 555® succinimidyl ester Protein Labeling Kit (Invitrogen, Frederick, Maryland) was used to fluorescently label fibrinogen for confocal microscopy of fibrin-microgel clots. Quant-iT™ Protein Assay Kit (Invitrogen, Frederick, Maryland) was used to analyze the amount of protein incorporated into the clot.

4.2.2 Fibrin Polymerization in the Presence of Microgels

Thrombin catalyzed polymerization of mixtures of fibrinogen and various fibrin knob peptide-labeled microgels (unfunctionalized microgels, GPRPFPAC-microgels, and GPSPFPAC-microgels) was initiated in transparent 96-well plates. In this assay, thrombin concentration dependent polymerization was observed for fixed concentrations of fibrinogen (1 mg/mL) and microgels (1 mg/mL, 2.5 mg/mL) with a fibrinogen-microgel to thrombin volume ratio of 9:1. The rationale for choosing 1 mg/mL and 2.5 mg/mL of microgels was in order to create a balanced effect of fibrin and microgels within the network. At lower microgel concentrations the network is dominated by fibrin and the effect of microgels is no longer significant. At higher microgel concentrations, the effect of microgels outweighs fibrin and the ability to form a fibrin network is hindered. Fibrinogen and microgel solutions were mixed and incubated together in HEPES + Ca buffer for 2 hours at room temperature and turbidity readings taken prior to adding various concentrations of human α-thrombin for a final thrombin concentration of

0, 0.01, 0.025, 0.05, 0.075, 0.1, 0.25, and 0.5 National Institute of Heath standard (NIH) units/mL. The clot turbidity at an absorbance of 350 nm was measured for 2 hours using a SpectraMax M2 Microplate Reader (Molecular Devices, Sunnyvale, CA) with readings taken every minute. From the turbidity curves, it was possible to determine the final turbidity of the mixture (normalized against controls without thrombin by subtracting initial turbidity without thrombin), and the clotting half time- the time taken for the clot to reach half the final normalized turbidity value at 2 hrs following thrombin addition. Each condition was tested with at least six samples.

4.2.3 Protein Incorporation into Fibrin-Microgel Clots

Following the turbidity assay, to determine the amount of unclotted protein, the clot was removed, and the isolated clot liquor was analyzed for total soluble protein using the Quant-iT™ Protein Assay. The Quant-iT™ protein reagent is highly selective for protein, with little protein-protein variability in the range of 0.25-5 ug. A working solution was prepared by diluting the Quant-iT™ protein reagent 1:200 in the provided buffer, and 200 uL of the solution added into each well of a black 96 well plate. 5 uL of each provided BSA standard was added to separate wells with duplicates of each concentration to create a standard curve by measuring the fluorescence at (Ex. 479/Em. 570 nm) using the BioTek Synergy H4 Hybrid Multi-Mode Microplate Reader (BioTek, Winooski, VT). 5 uL of the clot liquor from each sample was added to separate wells with duplicates of each in order to determine the amount of soluble protein in the clot liquor. The percent clottable protein was then back calculated from the amount of soluble protein in the clot liquor and normalized against controls without thrombin. Each condition was tested with at least six samples.

4.2.4 Exogenous Fibrinolysis of Fibrin-Microgel Clots

Fibrin-microgel clot degradation was evaluated using an exogenous fibrinolysis assay. Fibrin-microgel clots were prepared as in section 4.2.2 using a final thrombin concentration of 0.25 U/mL to allow the clots to reach their final turbidity at 2 hours. 100 uL of plasmin (0.5 U/mL) was overlaid on top of the fibrin-microgel clots and gently agitated at room temperature for 4 hours on an Eppendorf MixMate at 400 rpm. Every thirty minutes, turbidity readings were recorded at 350 nm using a SpectraMax M2 Microplate Reader (Molecular Devices, Sunnyvale, CA) and 5 uL samples from the clot liquor were taken to determine total soluble protein using the Quant-iT protein assay (see Section 4.2.3 for experimental details). The turbidity readings were normalized by subtracting the initial turbidity of the solution prior to thrombin addition. The percent soluble protein in the clot was calculated based on the theoretical maximum concentration of protein.

4.2.5 Confocal Imaging of Fibrin-Microgel Clot Structure

Fluorescently-labeled FIB-3 fibrinogen was prepared by conjugation to the amine reactive Alexa Fluor 555® succinimidyl ester following the manufacturer's recommended protocol. Clots containing 10% labeled fibrinogen were imaged using the Zeiss 510 laser scanning confocal microscope (Carl Zeiss, Thornwood, NY). Mixtures of 10 uL fibrinogen and 10uL microgels were preincubated in HEPES + Ca buffer for 1 hour prior to 20 uL thrombin addition, for a final concentration of 1 mg/mL fibrinogen, 0.25 U/mL thrombin, and 1 mg/mL, 2.5 mg/mL, and 5 mg/mL unfunctionalized, GPRPFPAC conjugated, or GPSPFPAC conjugated microgels. Following the addition of thrombin, the solutions were quickly mixed by pipetting and immediately added to a glass slide. The mixture was covered with a glass coverslip supported by 0.3 mm spacers on two sides. The open sides were sealed with nail polish to create a chamber, and the mixture was allowed to polymerize for 1hour before imaging. A 10 um Z-stack of 20

(0.53 um) slices under the 63X objective was captured for reconstructing the 3D fibrin network structure. At least 3 clots were formed independently for each condition, and 4 random sections were imaged per clot.

In order to visualize the interaction of the microgels in the fibrin network structure, 0.1 M 4-acrylamidofluorescein (AFA) labeled microgels were synthesized using the same method as for unlabeled microgel synthesis and were conjugated with peptides and incorporated into clots for confocal imaging shown in APPENDIX A.

4.3 Results

In this study, the ability of fibrinogen to trigger active knob peptide GPRPFPAC-microgel assembly was determined. In addition, the effect of microgels conjugated to active knob peptide (GPRPFPAC) or inactive control peptide (GPSPFPAC) and unfunctionalized microgels on fibrin polymerization was investigated. Clot turbidity and percent clottable protein measurements were performed using various concentrations of thrombin, with the readings normalized against controls without thrombin. All experimental groups were tested with at least two triplicate trials. There was a large variance in the results with fibrin polymerized in the presence of various fibrin knob peptide-microgels at different thrombin concentrations for significant statistical comparison. However general trends in the data are described in the sections below.

4.3.1. Fibrinogen-Triggered Microgel Assembly

Figures 6A and 7A of 1 mg/mL and 2.5 mg/mL microgel + fibrinogen solutions without the presence of thrombin show no change in turbidity due to microgel:fibrinogen interactions. A clear mixture is indicative of the absence of fibril assembly and clot formation. Additionally, these microgel + fibrinogen solutions resulted in no observable physical formation of a clot, but remained an aqueous solution even after a 2+ hour incubation of the microgels with fibrinogen. Interesting, the active knob peptide

GPRPFPAC-microgel containing clots do not increase the absorbance of the mixture as previously shown in another study [32], suggesting that the peptide-microgel conjugate concentration in solution is not enough to result in fibrinogen-microgel assembly arising from knob:hole interactions despite the multivalency of the microgels.

4.3.2 Fibrin-Microgel Clot Turbidity

4.3.2.1 Clot Turbidity Profiles

Turbidity curves for clots polymerized in the presence of 1 mg/mL microgels at various thrombin concentrations are presented in Figure 6. In Fig. 6B, for the 0.01 U/mL thrombin condition, delayed polymerization occurs for all microgel containing clots. This decrease in the polymerization rate indicates a competition effect of microgels altering the equilibrium rates of thrombin cleavage and fibrin monomer association at the low concentrations of thrombin. However, at thrombin concentrations of 0.025 U/mL and higher (Fig. 6C-H), the clots polymerized with microgels experience similar polymerization rates as the fibrin alone control, which indicates that at higher thrombin concentrations, the competitive effect of microgels is overcome to form a fiber network at similar rates. The effect of molecular crowding due to the microgels and the alteration in polymerization rate is explained further in the discussion section. In addition to a trend in polymerization rates, all clots polymerized in the presence of microgels observe a higher final turbidity. In general, an increase in clot turbidity indicates the formation of thicker fibrin bundles, whereas thinner fibrin bundles result in clear or glassy clots. This increase in clot turbidity suggests that thicker fiber bundles are formed in the presence of microgels.

Turbidity curves for clots polymerized in the presence of 2.5 mg/mL microgels at various thrombin concentrations are presented in Figure 7. In Fig. 7B- E, clots polymerized with 0.01-0.075 U/mL thrombin have delayed polymerization rates for all

microgel containing samples. This decrease in the polymerization rate for higher thrombin concentrations as compared to the 1mg/mL microgel conditions, can be attributed to the increased effect of competition by the microgels at higher concentrations. However, from 0.1-0.5 U/mL (Fig. 7F-H) the microgel containing clots experience similar polymerization as the control, suggesting that the rate of fibrin monomer formation to associate and form fibrils has overcome the competitive effect of the microgels. In addition, these clots result in higher final turbidity for all microgel conditions suggesting that while the polymerization rate is delayed, thicker fiber bundles are being formed.

Surprisingly, instead of observing increased rates of polymerization for the GPRPFPAC microgel condition, highly delayed polymerization rates are observed for low thrombin concentrations. In Fig 7B and 7C, at the 0.01 and 0.025 U/mL thrombin conditions, GPRFPAC microgels do not reach their final turbidity and display highly inhibited polymerization rates. This result reveals that the GPRPFPAC-microgels do not serve as nucleation sites for polymerization, but rather act as competitors with native fibrin monomers for polymerization into fibers. This result is corroborated by studies showing inhibition of fibrin polymerization by GPRP peptides and GPRP-PEG conjugates [5, 32]. However, at concentrations of 0.05 U/mL of thrombin and above (Fig. 7D-H) GPRPFPAC-microgels start to approach their final turbidity at 2 hours suggesting that at higher thrombin concentrations enough fibrin monomers are generated to overcome both competition due to microgels as well as competition of the peptide conjugated microgels for fibril formation.

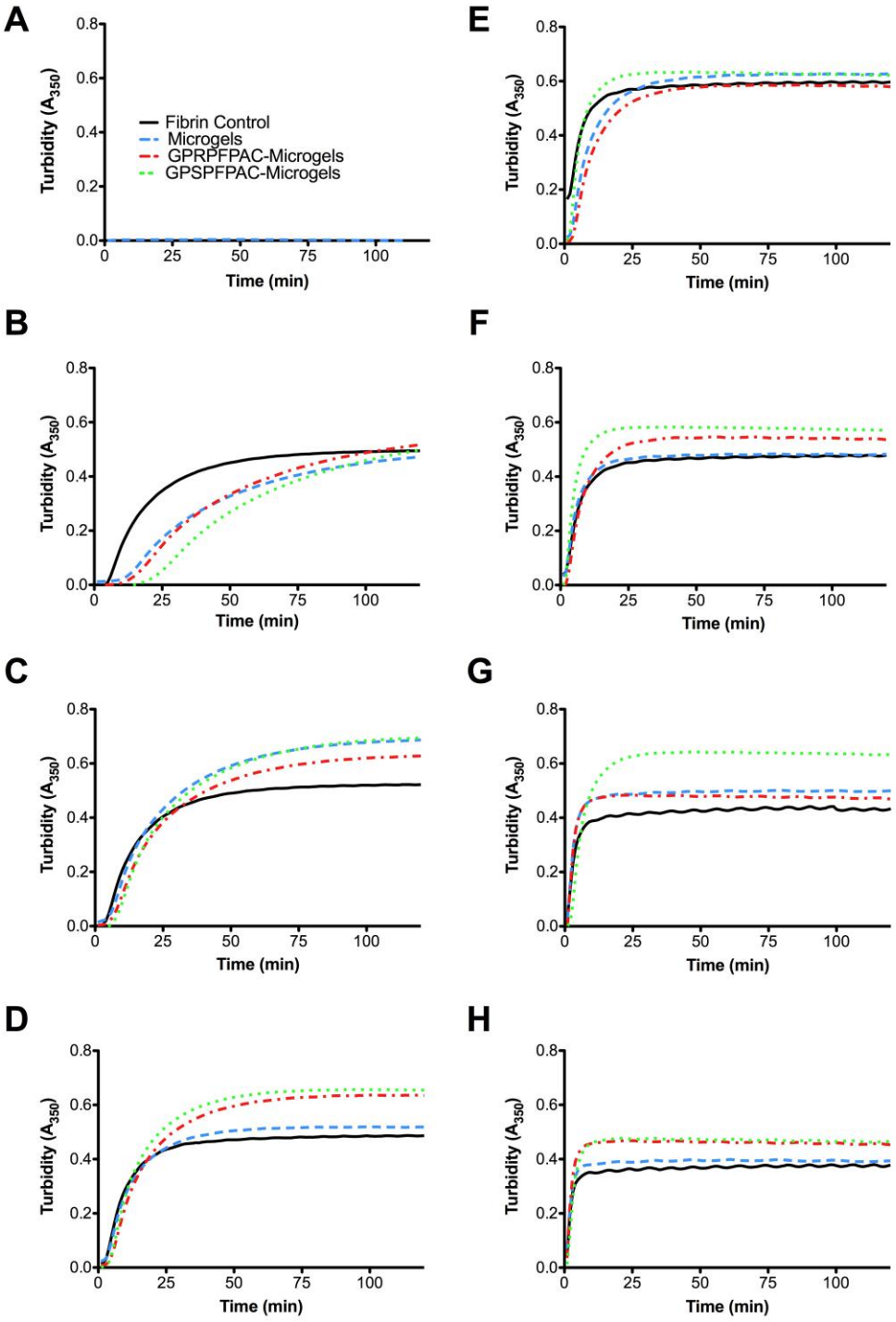

Figure 6. Turbidity Profiles of Fibrin Polymerized in the Presence of 1 mg/mL Microgels. 1 mg/mL fibrinogen polymerized for 2 hours in the presence 1 mg/mL of peptide labeled microgels (unfunctionalized microgels, GPRPFPAC-microgels, GPSPFPAC-microgels) at different thrombin concentrations - (A) No thrombin (B) 0.01 U/mL (C) 0.025 U/mL (D) 0.05 U/mL (E) 0.075 U/mL (F) 0.1 U/mL (G) 0.25 U/mL (H) 0.5 U/mL.

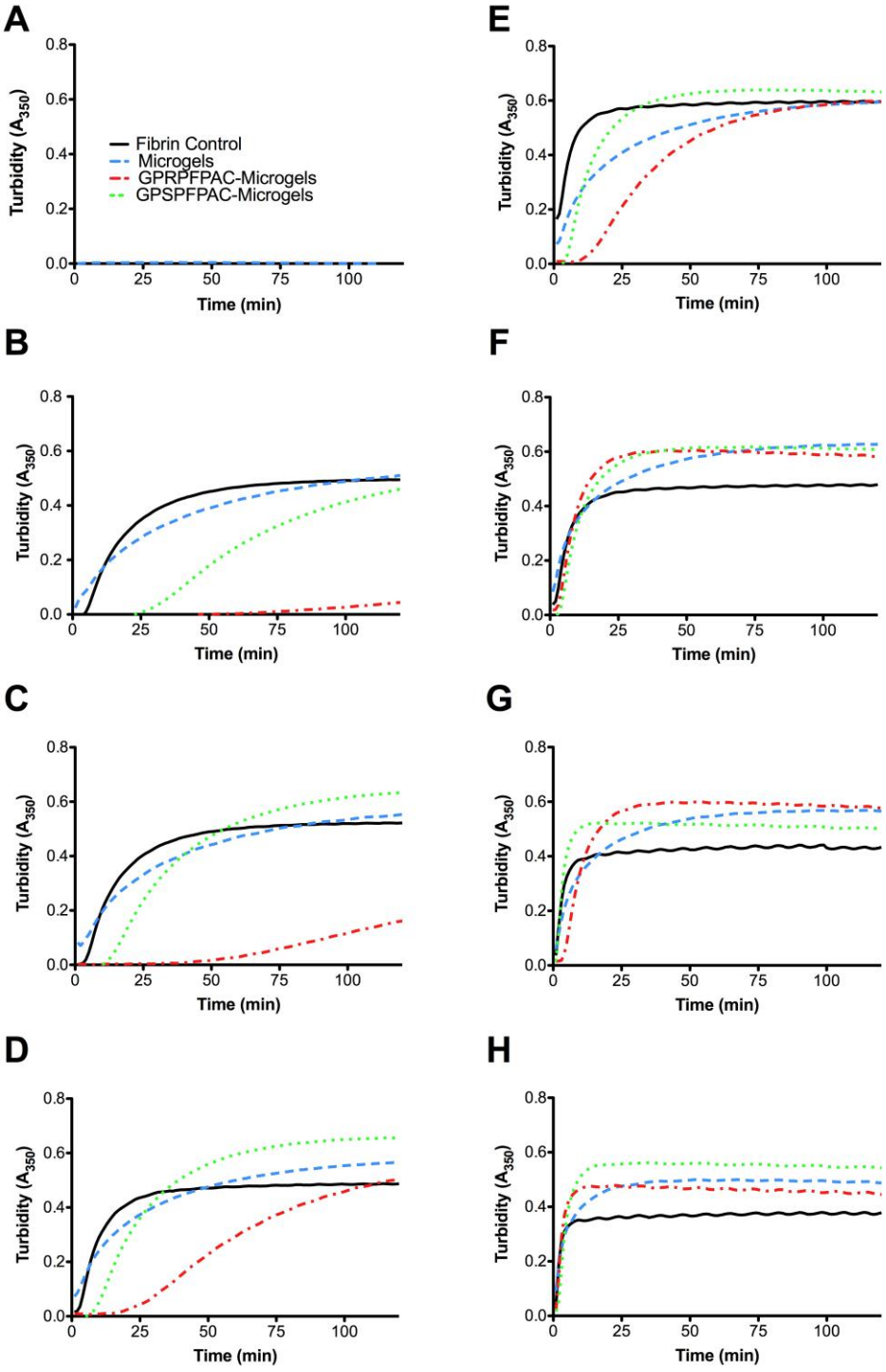

Figure 7. Turbidity Profiles of Fibrin Polymerized in the Presence of 2.5 mg/mL Microgels. 1 mg/mL fibrinogen polymerized for 2 hours in the presence 2.5 mg/mL of peptide labeled microgels (unfunctionalized microgels, GPRPFPAC-microgels, GPSPFPAC-microgels) at different thrombin concentrations - (A) no thrombin (B) 0.01 U/mL (C) 0.025 U/mL (D) 0.05 U/mL (E) 0.075 U/mL (F) 0.1 U/mL (G) 0.25 U/mL (H) 0.5 U/mL.

4.3.2.2 Final Clot Turbidity

The addition of microgels to the fibrin network seems to generally increase the final clot turbidity for thrombin conditions that result in similar polymerization rates as the fibrin control. This increase in final turbidity suggests the formation of thicker fiber bundles, possibly due to macromolecular crowding by the microgels. The effect of macromolecular crowding on fibrin polymerization is explored in more detail in the discussion. In Fig. 8A, clots polymerized with 1mg/mL microgels with different thrombin concentrations all reach final clot turbidity at the end of 2 hours. However in the 2.5 mg/mL microgel condition, GPRPFPAC-microgels do not reach final clot turbidity at 0.01 and 0.025 U/mL (Fig. 8B). It only approaches final clot turbidity at 0.05 U/mL and above. Interestingly, the overall trend shows that clots polymerized with GPSPFAC-microgels have the highest overall clot turbidity, which indicates the formation of thicker fiber bundles. In addition, final clot turbidity does not change much for unfunctionalized microgels at different thrombin concentration and appears to be lower than other microgels for all conditions, which indicates the formation of thinner fibers than all the other microgel conditions. While the reason for the difference in final turbidity between different peptide-microgel conjugates is uncertain, it is possible that microgel charge plays an important role in fibrin polymerization by altering fibril formation, structure, and organization. The effect of microgel charge on fibrin polymerization is further explored in the discussion section.

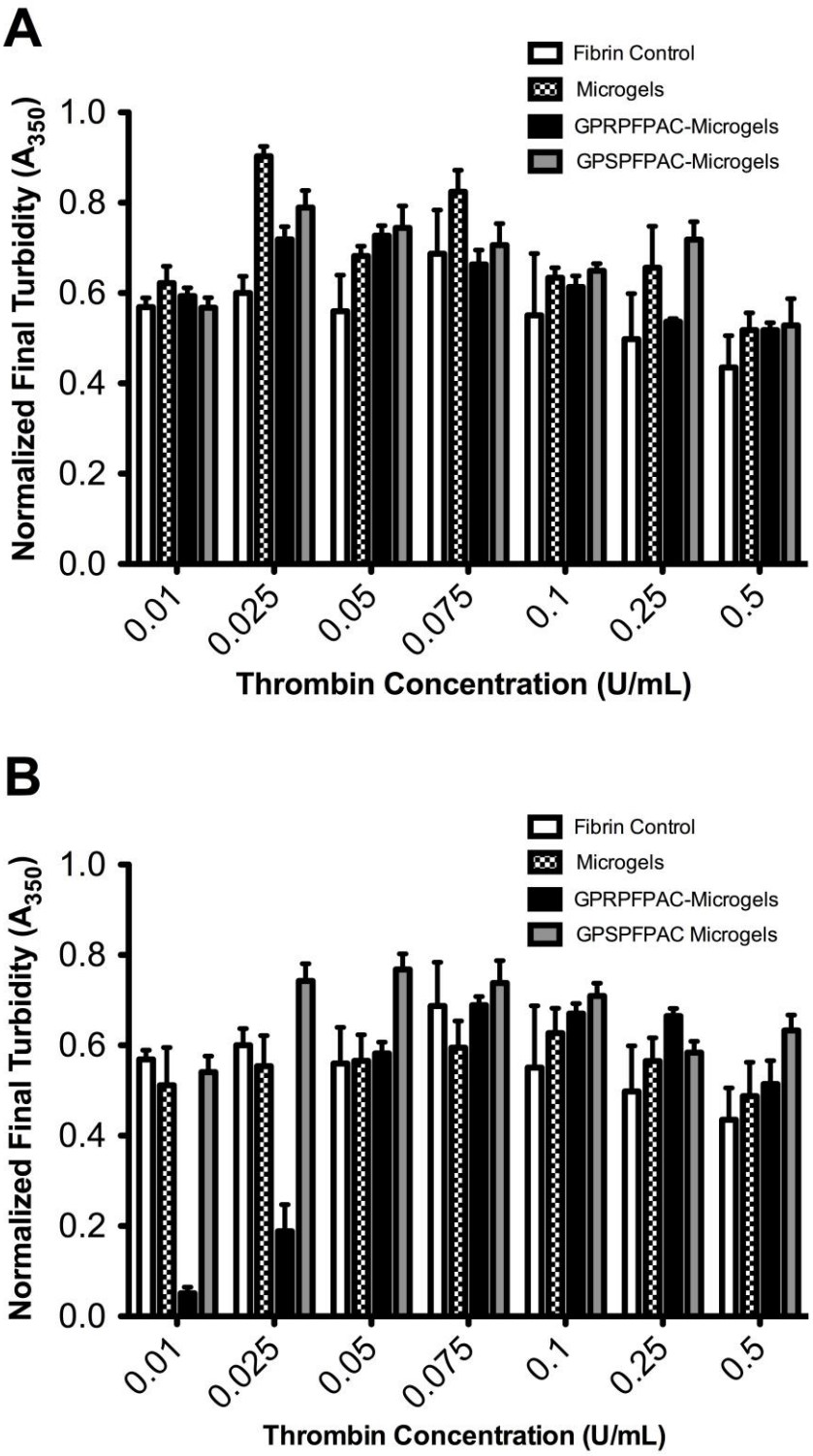

Figure 8. Final Turbidity of Fibrin-Microgel Clots. Final turbidity values of fibrin-microgel clots after polymerizing for 2 hours, normalized against controls without thrombin. (A) clots polymerized with 1 mg/mL microgels (B) clots polymerized with 2.5 mg/mL microgels.

4.3.2.3 Clotting Half-Time

The clotting half time as defined by the time needed to reach ½ the normalized final turbidity value at 2 hours, was only calculated for clots reaching final turbidity after 2 hours of polymerization shown by * in Figure 9. The clotting half-time for clots polymerized with 1 mg/mL microgels is shown in Fig. 9A. There is a thrombin concentration dependent response where the clotting half-time is greater for clots containing microgels polymerized with low concentrations of thrombin (less than 0.1 U/mL). This impedance of rapid fiber formation is likely due to the competetive effect of microgels altering equilibrium rates of fibrin monomer formation and association for network formation. At 0.1-0.5 U/mL thrombin, the clotting half-time for all microgel containing clots approaches the same time as the control suggesting that at high thrombin conentrations, sufficient fibrin monomers are generated to overcome the competitive effect of microgels. The clotting half-time for clots polymerized with 2.5 mg/mL microgels is shown in Fig. 9B. The same trend is observed for GPFPFAC-microgels and GPRPFPAC-microgels at this concentration as the 1 mg/mL condition that at low thrombin concentrations there is an increased delay in polymerization rate from 0.01-0.075 U/mL thrombin and even slightly at 0.1 and 0.25 U/mL thrombin. GPRPFPAC-microgels greatly increased the clotting half-time up to 0.075 U/mL and did not reach final turbidity for the 0.01 and 0.025 U/mL thrombin conditions. Interestingly, the 2.5 mg/mL unfunctionalized microgel condition did not vary greatly from the fibrin alone control for all thrombin concentrations. This difference from the non-binding GPSPFPAC-microgel control could be due to differences in microgel charge, explained in the discussion section. GPSPFPAC- microgels at 2.5 mg/mL display similar trends as the 1mg/mL condition but much more pronounced with longer clotting half-times. The results from the polymerization data show that there is a balance between thrombin, microgel, and active fibrin knob peptide concentration in order to achieve clots without significantly altered polymerization rates.

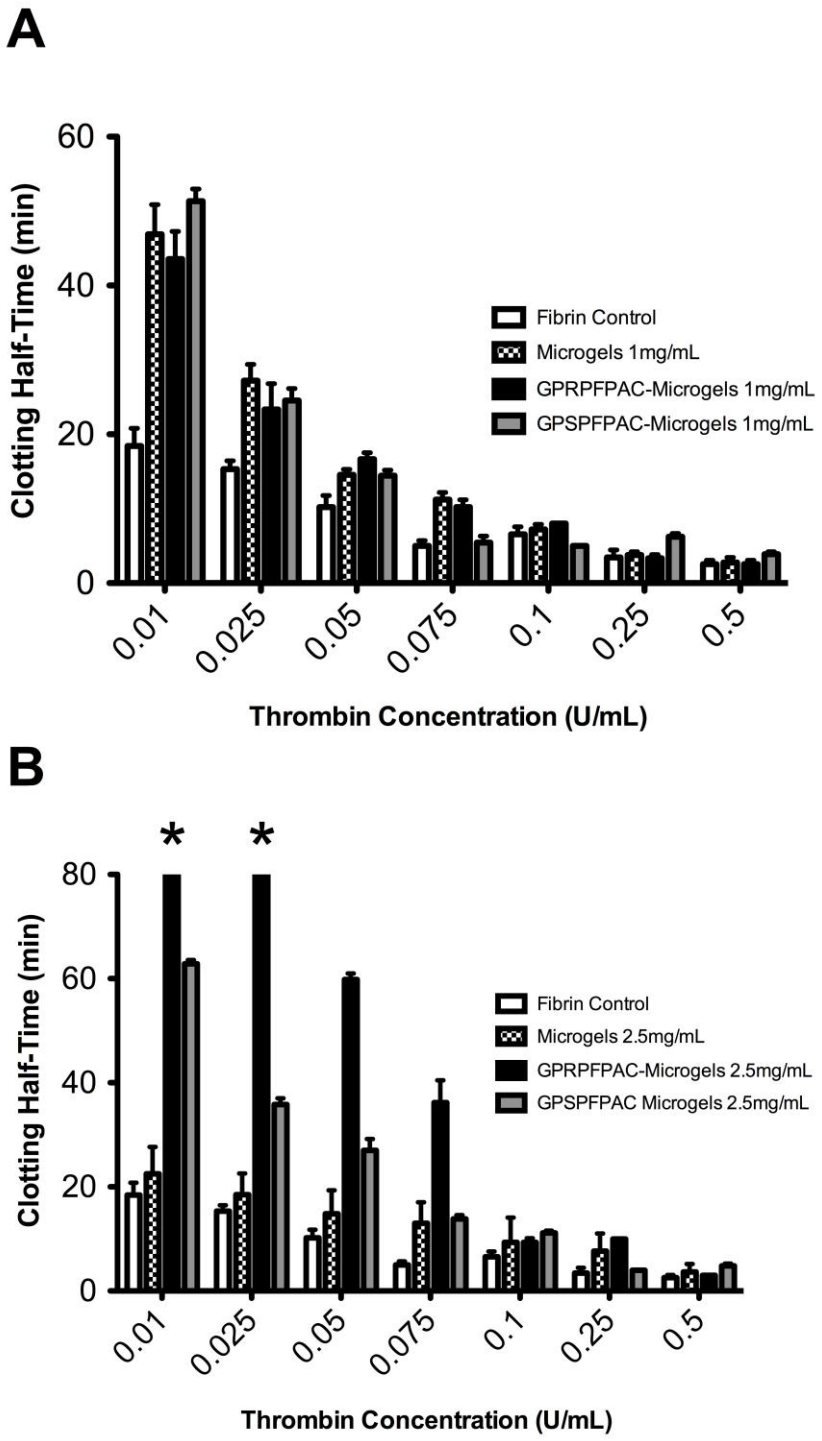

Figure 9. Clotting Half-Time of Fibrin-Microgel Clots. Clotting half-time, measured as the time to reach ½ the normalized final turbidity value at 2 hours for various fibrin-microgel clots polymerized with different thrombin concentrations. (A) clots polymerized with 1 mg/mL microgels (B) clots polymerized with 2.5 mg/mL microgels. * denotes 2.5 mg/mL GPRPFPAC-microgel containing clots polymerized with 0.01 U/mL and 0.25 U/mL thrombin that did not reach final turbidity at 2 hours.

4.3.3 Percent Clottable Protein in Fibrin-Microgel Clots

The percent clottable protein in clots polymerized with 1 mg/mL microgels is shown in Figure 10A. The clots containing higher microgel concentrations polymerized with low concentrations of thrombin (< 0.1 U/mL) contain less clotted protein after 2 hours of polymerization. At the 0.01 U/mL thrombin condition, the clots with GPSPFPAC-microgels have the least amount of clottable protein. It is uncertain why clots with the non-binding GPSPFPAC-microgels at 1 mg/mL have the highest overall turbidity, but the least amount of clottable protein compared to the fibrin control and other microgel conditions. GPRPFPAC-microgels at 1 mg/mL display similar amounts of percent clottable protein as the control at all thrombin concentrations. Clots with GPSPFPAC-microgels and unfunctionalized microgels have decreased amounts of protein at all thrombin concentrations. At the 0.25 U/mL thrombin condition, control clots have 95% clottable protein, GPRPFPAC-microgel containing clots have 95%clottable protein, GPSPFPAC-microgel containing clots have 87% clottable protein, and unfunctionalized microgel containing clots have 89 % clottable protein. Formidable fibrin clots are considered to have at least 90% clottable protein, indicating that the presence of 1 mg/mL microgels approaches the acceptable limit for a formidable fibrin clot [15].

The percent clottable protein in clots polymerized with 2.5 mg/mL microgels is show in Figure 10B. For the 0.01-0.05 U/mL thrombin condition GPRPFPAC-microgel containing clots display the least amount of clottable protein because the clots have not reached final turbidity. From 0.075 U/mL and above, GPRPFPAC-microgels display similar trends as the 1 mg/mL condition with higher percent clottable protein that the other microgel conditions but containing slightly less percent clottable protein than the 1 mg/mL condition. At the 0.25 U/mL thrombin condition, control clots have 95% clottable protein, GPRPFPAC-microgel containing clots have 88%clottable protein, GPSPFPAC-microgel containing clots have 79%

clottable protein, and unfunctionalized microgel containing clots have 74 % clottable protein. This suggests that while the polymerization of GPRPFPAC-microgel containing clots is delayed, there is greater retention of protein in these clots than with other microgel containing clots. A similar trend of the least amount of percent clottable protein is observed for the 2.5 mg/mL GPSPFPAC-microgel condition at 0.01 U/mL thrombin. It is uncertain why the GPSPFPAC-microgels cause less protein retention in the final clot, but it is possible that the differences are because of alterations in macromolecular crowding due to differences in microgel charge, explained in the discussion. The general trend from the percent clottable protein data shows that at increasing microgel concentrations less protein is incorporated into the clot due to volume exclusion by the microgels.

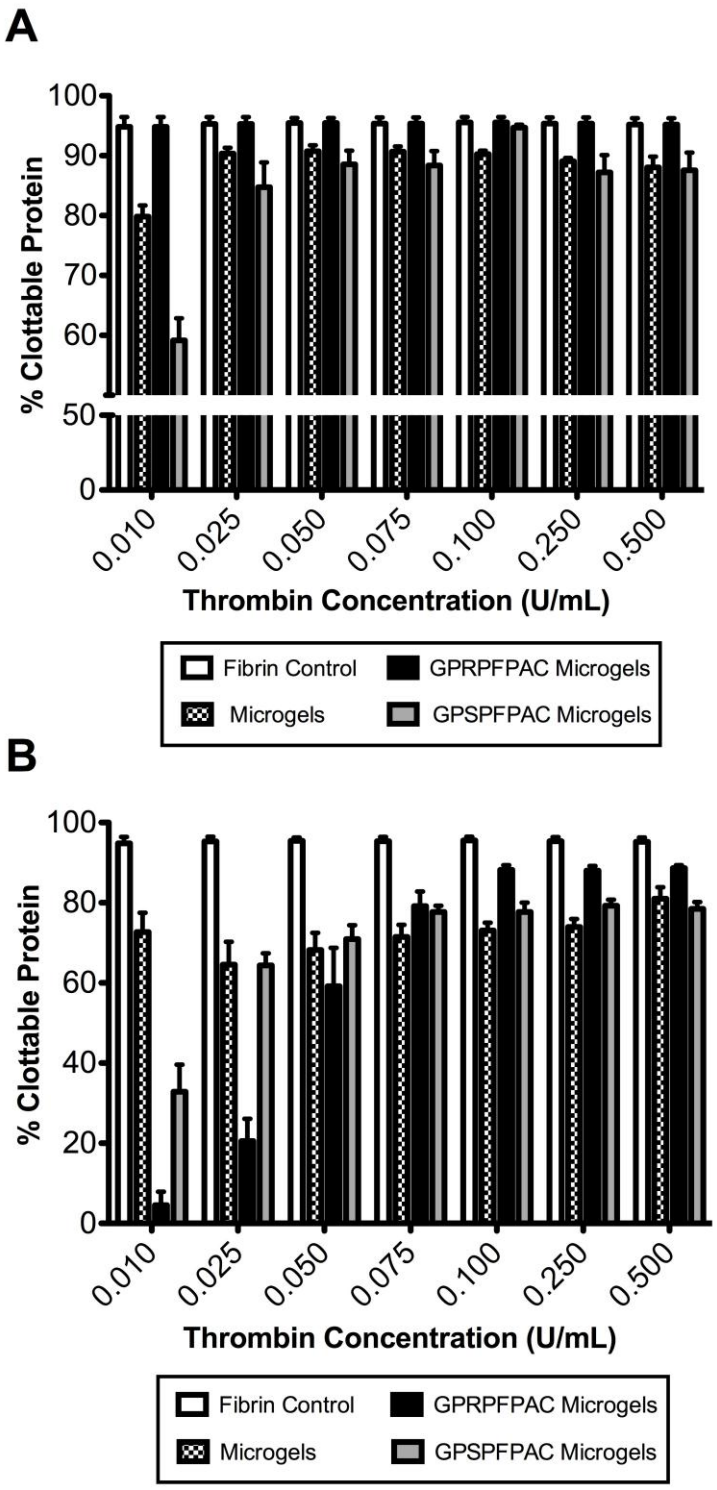

Figure 10. Percent Clottable Protein in Fibrin-Microgel Clots. Percentage of clottable protein was evaluated 2 hours after initiating polymerization for (A) 1 mg/mL microgel-fibrin gels and (B) 2.5 mg/mL microgel-fibrin gels by back-calculating from the amount of soluble protein in the clot liquor of extracted clots, normalized against controls without thrombin.

4.3.4 Degradation of Fibrin-Microgel Clots

Clot degradation profiles of fibrin-microgel gels reveal that the clots degrade at a more rapid rate with increasing concentrations of microgels. The degradation of clots polymerized in the presence of 1 mg/mL microgels (Fig. 11A) shows that all clots containing microgels experience similar degradation rates. However, these rates are all slightly fast than the control as observed by the slopes of the curves. The degradation of clots polymerized in the presence of 2.5 mg/mL microgels (Fig. 11B) have similar characteristics as the 1 mg/mL condition where the degradation rates of all microgel containing clots are similar to one another. However, the 2.5 mg/mL microgel containing clots experience even quicker degradation rates than the 1 mg/mL condition. Because exogenous fibrinolysis is a diffusion dependent process, these results are not surprising considering that the volume filling microgels are expected to increase the porosity of the resulting network at increasing concentrations. Previous studies have shown similar trends, indicating that active knob peptide-PEG conjugates increased the effective diffusion coefficient through a fibrin network by 50-70% compared to control gels [15].

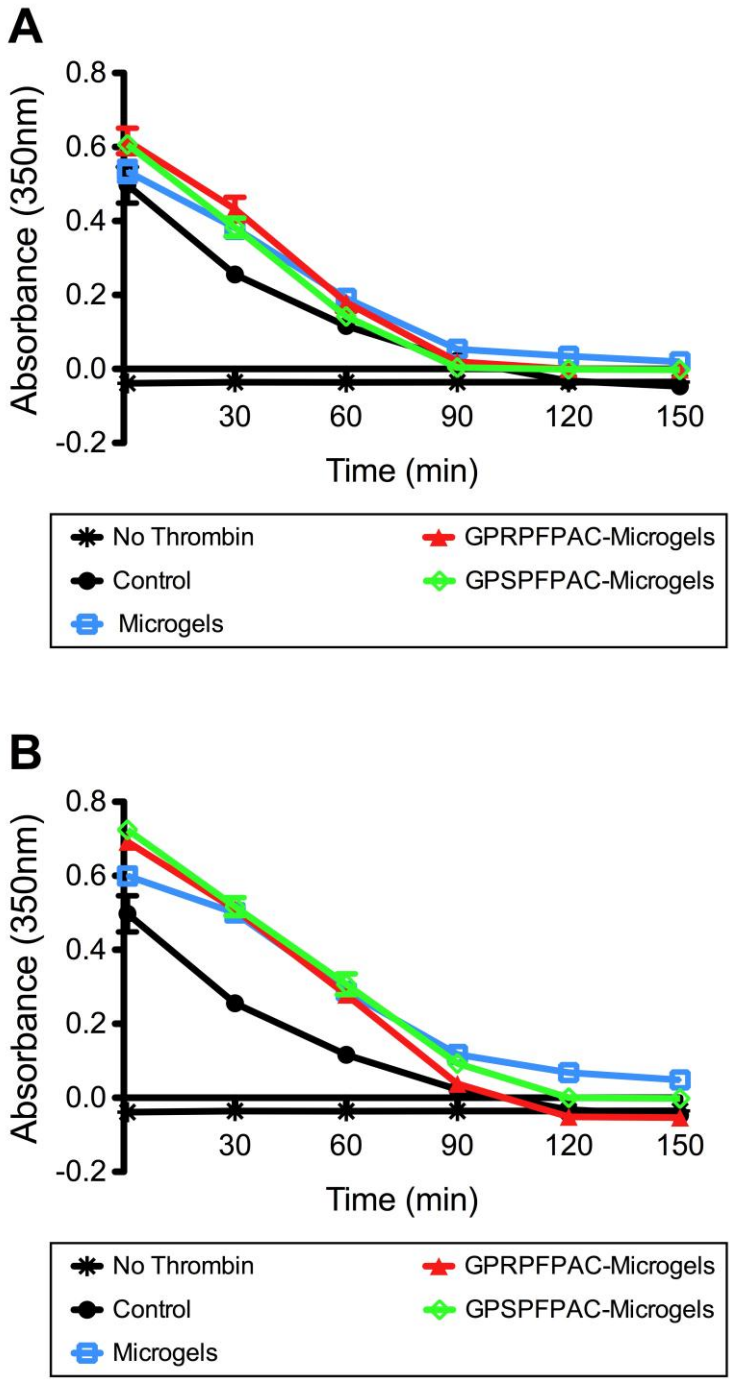

Figure 11. Turbidity Profiles of Fibrin-Microgel Clot Degradation. Absorbance measurements of clot degradation at 350 nm. (A) Exogeneous fibrinolysis of 1 mg/mL fibrin gels polymerized in the presence of 1 mg/mL microgels. (B) Exogeneous fibrinolysis of 1 mg/mL fibrin gels polymerized in the presence of 2.5 mg/mL microgels.

The percent soluble protein of fibrin-microgel clots after plasmin addition (Figure 12) displayed similar results as the clot degradation profiles where the clots containing higher concentrations of microgels resulted in more rapid rates of degradation. For clots containing 1mg/mL microgels (Fig. 12A), similar percent soluble protein was observed for peptide-functionalized microgels and control clots. Although the initial amount of soluble protein for unfunctionalized microgel containing clots was higher, the degradation rate appears to be roughly the same for all groups. For clots containing 2.5 mg/mL microgels (Fig. 12B), similar percent soluble protein was observed for peptide-functionalized microgels and control clots. For clots containing 2.5 mg/mL unfunctionalized microgels, the initial amount of soluble protein was higher than other conditions. This is supported by the percent clottable protein data for 2.5 mg/mL unfunctionalized microgels polymerized with 0.25 U/mL thrombin showing the least amount of clottable protein compared to all other groups (Fig.10B). Additionally, these clots appear to degrade at a slightly faster rate within the first thirty minutes after plasmin addition. These results suggest that the presence of microgels alters fibrin network structure causing an increased susceptibility of clots to fibrinolysis.

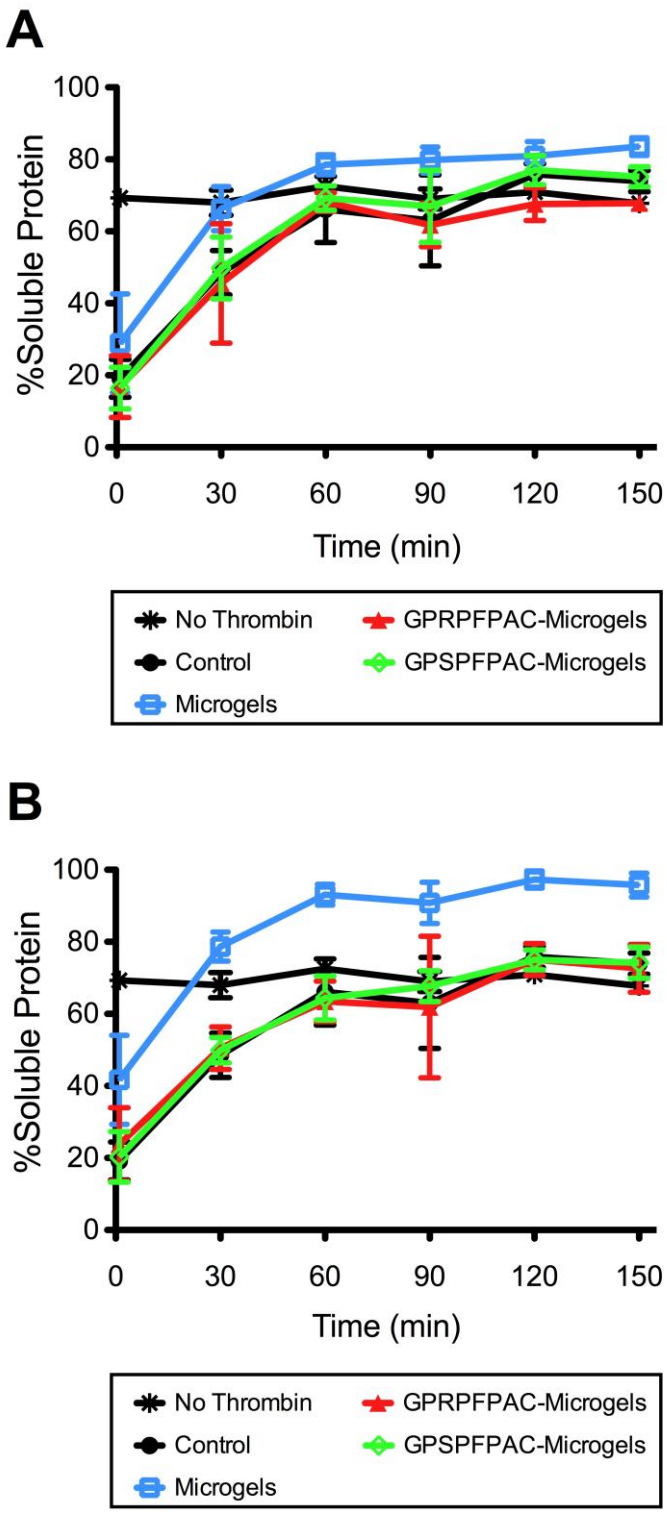

Figure 12. Percent Soluble Protein of Degrading Fibrin-Microgel Clots. (A) Percent soluble protein of 1 mg/mL fibrin clots polymerized in the presence of 1 mg/mL microgels. (B) Percent soluble protein of 1 mg/mL fibrin clots polymerized in the presence of 2.5 mg/mL microgels.

4.3.5 Fibrin-Microgel Clot Structure

For a more direct evaluation of the type of structural changes to a fibrin network imposed by the presence of various peptide-microgel conjugates, 1 mg/mL clots were formed on glass slides using 10% Alexa Fluor 555-labeled fibrinogen to enable direct visualization and imaging of microgel containing clots using confocal microscopy (Fig. 13). Clots containing 1 mg/mL unfunctionalized microgels appeared similar to the control but appeared to have slightly thinner fibers (Fig. 13B). Clots containing 1 mg/ml GPRPFPAC microgels had shorter more branched fibers than the fibrin control (Fig. 13C), and the clots containing 1 mg/ml GPSPFPAC microgels had longer slightly thinner fibers than the GPRPFPAC-microgel condition, but appear more similar to the fibrin only condition but with thicker fibers than the control (Fig. 13D). With the unfunctionalized microgels, at increasing concentrations of microgels there appears to be increased fiber deposition compared to the control, but result in clots with highly thin fibers (Fig. 13B, E, H). This reduction in fiber thickness as compared to clot containing other types of microgels can explain why the final turbidity for unfunctionalized microgels is lower than the peptide-conjugated microgel conditions. GPRPFPAC-microgels at the 2.5 mg/mL concentration (Fig. 13F), display the same short, thicker, highly branched fibers and the GPSPFAC-microgels (Fig. 13G) have similar long-thicker fibers as the 1 mg/mL conditions but with reduced total fiber volume. Interestingly, at the highest microgel concentration containing 5 mg/mL GPRPFPAC-microgels (Fig. 13I), clots displayed nodular like structures with a greatly reduced total fiber volume than the control. One possible explanation for the nodular structures is the formation of fibrin-microgel aggregates where the local concentration of GPRPFPAC peptide available for association with fibrin holes is high. The 5 mg/ml GPSPFPAC-microgel condition (Fig. 13J) had a similar long-thick fiber structure as the 1mg/ml sample but with greatly reduced total fiber volume. One reason for the great difference in structure between the GPSPFPAC-

microgels and the unfunctionalized microgels is possibly due to the charge difference of the microgels, which will be further explored in the discussion section.

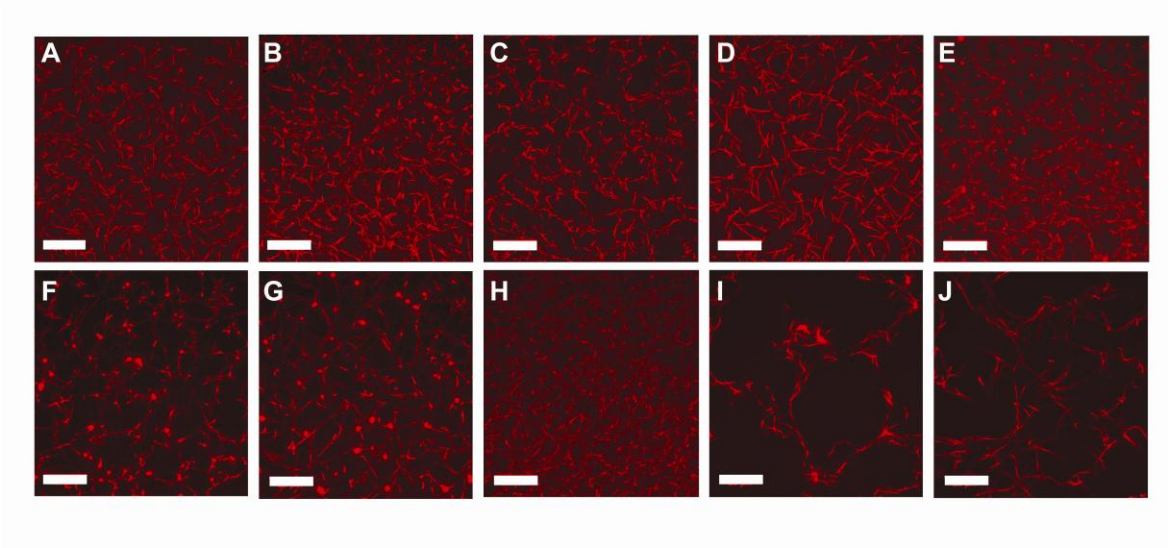

Figure 13. Confocal Z-stack Images of Fibrin Network Structure of Microgel Containing Clots. 1 mg/mL fibrin clots polymerized for 1 hour in the presence of peptide-labeled microgels at different concentrations (1 mg/ml, 2.5 mg/mL, and 5 mg/mL respectively). (A) Fibrin control. (B, E, H) Clots containing unfunctionalized microgels (C, F, I) Clots containing GPRPFPAC-microgels. (D, G, J) Clots containing GPSPFPAC-microgels. Scale bar = 20um.

4.4 Discussion

The result from the turbidity readings and physical determination of fibrinogen-triggered microgel assembly show that at the concentrations of microgels and fibrinogen and the peptide labeling density used, a colloidal gel was not able to form. Turbidity measurements are traditionally used to measure fiber network formation by the change in absorbance, but because our system does not depend on the formation of fibers, turbidity measurements are not the most suitable determination of the formation of a gel network. It is possible that at the concentrations of microgels, peptide, and fibrinogen we explored, the formation of clear or glassy micro-aggregates of fibrinogen coated microgels occur. A better detection system probing the interactions at the single molecule level, such as surface plasmon resonance (SPR) measurements to determine the kinetic binding

coefficients of fibrinogen with peptide-labeled microgels, needs to be explored. Dynamic light scattering techniques are also potential methods that can be used to probe the interactions of active knob peptide-labeled microgels with fibrinogen.

The general trends from the fibrin polymerization data show that fibrin polymerized in the presence of microgels leads to overall greater final turbidity than the control, and at low thrombin concentrations, the rate of polymerization is delayed with increasing concentrations of microgels. GPRPFPAC-microgels have an increased delay in polymerization compared to other microgel conditions likely due to competition of active knob peptides with fibrin monomers for polymerization hole domains. In addition to the delayed polymerization rates, the amount of protein incorporated within a fibrin network is decreased with increasing concentrations of microgels. Correspondingly, the degradation assays of fibrin-microgel gels revealed that with increasing concentrations of microgels, the clots degraded at a more rapid rate. Confocal microscopy of microgel containing clots reveals greatly altered fibrin network structure. Peptide labeled-microgels at increasing concentrations led to the formation of clots with highly open and porous networks, however, unfunctionalized microgels led to the formation of highly dense thin fiber meshes. The possible explanations for these trends are explored in the discussion sections below.

4.4.1 Peptide Ligand Density

As mentioned in the discussion of chapter 3, the low percent yield of peptide conjugation to microgels suggests a heterogeneous display of peptides off the surface of the microgel. Homogeneous conjugation and ligand density are crucial parameters determining interaction with fibrinogen and subsequent assembly of microgels into a colloidal gel. In order to better control peptide ligand density, an alternate conjugation approach should be used to greatly increase the percent yield. In order to determine the effect of ligand density on fibrinogen triggered colloidal assembly, microgels with up to

20% AAc groups available for conjugation should be used as an alternate to 5%AAc microgels. By varying the percent of acid groups conjugated with peptides from 0-100% functionalized, it will be possible to study the effect of ligand density on fibrinogen triggered microgel assembly in order to determine the optimal conjugation ratio for the rapid formation of a gel network. Although one possible downside to increasing the AAc concentration is that acrylic acid is extremely toxic to cells, and would not be the best material of choice for tissue engineering and regenerative medicine applications. Alternatively, more biocompatible materials might present a better option for peptide-fibrinogen knob:hole interaction facilitated hydrogel formation. The peptide density, the microgel concentration, and fibrinogen concentration are critical parameters that need to be optimized to ensure that fibrinogen molecules are more likely to bind between two microgels rather than binding to peptides on the same microgel in order to form a colloidal assembly.

Fibrin polymerization in the presence of knob peptide-labeled microgels is dependent upon peptide, microgel, and thrombin concentration incorporated into the clot. It has been shown that at peptide concentrations of 100-fold molar excess to fibrinogen, that clot polymerization is inhibited, but at lower molar ratios fibrinogen is "pre-engaged" through knob:hole interactions with the peptide to alter polymerization rates and the resulting composition and structure [32]. In the present study, fibrin polymerization assays used a 1mg/mL concentration of fibrinogen, which is approximately 2.94 mM. For the peptide-functionalized microgels at a 1 mg/mL concentration, a GPRPFPAC peptide concentration of 0.0145 mM per mg/mL of microgel and a GPSPFPFAC peptide concentration of 0.081 mM per mg/mL of microgel, correspond to a 1:200 mol ratio and 1:36 mol ratio of peptide to fibrinogen, respectively. These ratios are much lower than the 100:1 molar excess necessary for complete inhibition of clot formation, and suggest that free fibrinogen molecules not "pre-engaged" with active peptides are available for polymerizing into a fiber network.

In this study, the effect of microgel concentration on fibrin polymerization is dominant over the effect of peptide concentration. Based on previous studies of peptide: fibrinogen ratios on clot polymerization, it is possible that peptide ligand density equivalent to 100:1 molar ratio of peptide to fibrinogen for a 1 mg/mL concentration of microgels is sufficient to form a colloidal assembly, and enough to completely inhibit clot formation in the presence of clotting enzymes. In a previous paper on knob peptide-PEG conjugates, it was shown that tetravalent peptide-PEG conjugates in a 1:1 mol ratio of conjugate to fibrinogen had the greatest impact on fibrin matrix structure through the formation of a hybrid assembly where each peptide-PEG conjugate interacts with 4 fibrinogen molecules, while each fibrinogen molecule has 4 holes available to participate in knob: hole interactions with other peptide-PEG conjugates [32]. This is a highly controlled system in which the molar ratios of peptide to fibrinogen can be readily adjusted based on conjugate valency. Future studies will aim to achieve this level of control with peptide-conjugated microgels by using better techniques for more efficient conjugation and investigating the effect of peptide ligand density on microgel interactions with fibrinogen.

4.4.2 Microgel Shape

While the round spherical shape of microgels did not greatly hinder the formation of a fibrin network, it did not assist in the formation of a fibrin network like we had hoped. The large difference in the shape and size of a microgel as compared to a fibrinogen molecule or fibrin monomer can be partially attributed to why we did not observe a decrease in the rate of fibrin polymerization. Future generations of knob peptide-polymer conjugates should take into consideration the shape and size scale of a typical fibrin monomer or fibrin fibers to assist in the formation of a fiber network. Exploring the use of polymers with rod-like shapes that resemble a fibrin fiber in shape and size might be the next step in rationally designing a knob peptide-polymer conjugate

that will assist in the self-assembly of fibrin fibers into a matrix. Based on the results of previous studies using peptide-PEG conjugates, it was suggested that the design of bisbivalent peptide-PEG linkers could favor the formation of course networks of thick fibers by pinning the ends of fibrinogen molecules together through knob: hole interactions to form protfibril-like structures, even in the absence of clotting enzymes [32]. Using a similar concept, Joel H. Collier's group investigates the use of fibrin-based peptides and peptide-polymer conjugates for the formation of self-assembling viscoelastic hydrogels [31]. Short peptides from the coiled-coil domain of fibrin were conjugated to short PEG chains to form triblock peptide-PEG copolymers which then self-assemble in appropriate buffers to form a hydrogel. Similar self-assembly approaches utilizing the size and shape of native fibrin fibers should be explored for the next generation of knob peptide-polymer conjugates.

4.4.3 Macromolecular Crowding

The molecular weight of the macromolecule being polymerized into a fibrin network has a significant influence on the final structure and physical properties of the matrix. In one study, turbidity measurements and microscopy indicated that fibrin polymerized in the presence of low molecular weight heparin led to a more transparent rigid network with thin fibrin bundles, whereas the presence of unfractionated heparin resulted in opaque more porous networks with thick fibrin fibers [23]. For fibrin knob peptide conjugates, a biphasic effect of PEG chain length on fibrin polymerization was reported, where increased inhibition of fibrin polymerization occurred with active knob peptide-PEG conjugates from 0 to 5 kDa PEG, but above 5 kDa anticoagulant activity was diminished. For bivalent and tetravalent peptide-PEG conjugates, the results indicate that the presence of larger conjugates (7.5 kDa, 10 kDa, and 20 kDa GPRPx-PEG) favored the formation of stable, fine highly branched networks [32]. Additionally, the

formation of tight nodules of protein in GPRP-PEG conjugates but not in their respective controls is possibly attributed to clusters of GPRP-PEG-bound fibrin(ogen). This suggests that larger conjugates with long mobile PEG chain linkers between the peptide knobs interfere with lateral aggregation of fibrin protofibrils to form thick fibers [32], possibly due to non-directional orienting of fibrin molecules mediated by knob:hole interactions prior to thrombin addition [32]. Considering that the molecular weight of ULC microgels is expected to be between 10^6 and 10^9 g/mol [47, 48], the effect of microgel molecular weight is drastically multiplied as compared to PEG or heparin incorporation into a network. The expected result, based on these data is the formation of highly open and porous networks with very thick fibrin fibers or tight fiber clusters. This could explain why the final turbidity of fibrin polymerized in the presence of microgels is higher than the control and is further confirmed by the 5 mg/mL peptide-labeled microgel condition with the highly open network with thick fibers. However, the unfunctionalized microgel condition is an anomaly with its increased fiber deposition at higher concentrations. It is uncertain why this effect occurs, but it is possible that charge interactions play a large role in polymerization and fibrin deposition which will be further explored in the next discussion section.

An explanation for the effect of microgel concentration and molecular weight on fibrin polymerization and structure can be partially attributed to macromolecular crowding (MMC). MMC is a biophysical concept in which inert macromolecules in solution occupy a significant volume of the medium and subsequently impact the biochemical reactions both *in vivo* and *in vitro* [63]. Inert macromolecules limit the space available for the reactant molecules by occupying space and creating dead space in between macromolecules that the reactant molecules are unable to pass through. Both macromolecule volume and dead space volume contribute to the exclude volume unavailable for reactant molecules, which result in two possible outcomes on the reactant molecule [64]. Firstly, the reduction in volume available for reactant interaction increases

the effective concentration of the reactant molecules and hence the thermodynamic activity of the reactant. Secondly, the diffusion rate and rate of encounter of the reactant molecules with one another is reduced [65]. The first will result in increased reaction rates, while the second will result in decreased reaction rates [66].

The effect of macromolecular crowding on extracellular matrix deposition has been explored by Krysten Van Vliet's group, and their studies have shown that the addition of inert macromolecules was able to enhance collagen deposition *in vitro* by increasing the effective activities of two key enzymes involved in collagen deposition [67]. Another group found that either the presence of 500 kDa dextran sulfate or PEG increased the respective activities of purified procollagen C-proteinase and procollagen N-proteinase in vitro in a cell free system [68].

Based on these results, it is possible that our fibrin-microgel system creates a delicate balance between increased effective thrombin activity and reduced fibrin monomer-monomer association to form fibers. While turbidity measurements are not the best measure of increased effective activity of thrombin, the MMC effect of microgels inhibiting fibrin monomer association to form fibers is observed by the delayed polymerization rates with increasing concentrations of microgels. In addition to the effect of microgel MMC, the active knob peptide (GPRPFPAC)-microgels are not an inert part of the system, but actively compete with fibrinogen and fibrin monomers for knob holes, and further delay fibrin polymerization.

One thing to note regarding the effect of macromolecular crowding, is that most molecular crowders are relatively solid masses, whereas ULC microgels are expected to be extremely porous due to their ultra-low degree of cross-linking and formation of a highly loose chain network. In order to determine the MMC effect of microgels, it will be important to determine the pore size and diffusivity of a microgel and examine whether ions, or even proteins can pass through an individual microgel. Microgel concentration, pH, ionic strength, and temperature are all critical conditions that will influence microgel

pore size and diffusivity. The degradation results suggest that diffusion is not hindered by the presence of microgels, but rather perpetuated by the microgels. Whether this is because of perturbations to a fibrin network with increased porosity due to volume exclusion by microgels, or whether this is due to direct diffusion through the microgels is uncertain. The mechanism of fibrin-microgel clot degradation needs to be investigated further in future studies.

4.4.4 Microgel Surface Charge

In addition to the size of the macromolecular crowder, surface charge of the macromolecule plays a large role in contributing to the excluded volume occupied by the crowder [64]. For anionic macromolecules, the surface charge adds a hydration shell around the molecule and contributes to steric exclusion due to like-charge repulsion increasing the effective volume of the crowder. The study by Raghunath et al, found a marked increase in collagen deposition with a negatively charged 200 kDa polysodium-4-styrene sulfonate macromolecule. This difference in charge on MMC and ECM deposition possibly plays a large role in our fibrin-microgel system. Unfunctionalized microgels are functionalized with 5% AAc that carry a negative charge in physiological pH, while the GPSPFPAC peptide has a neutral charge, and the GPRPFPAC peptide has a positive charge of +1 [11]. While the percent of peptide conjugated to the microgels is low, it is possible that the slight differences in charge are sufficient to affect the polymerization of fibrin in different ways. What the exact effect or interaction of charged microgels with fibrinogen is unclear. In order to determine whether there is a true difference in charge between the microgels used in this study, unfunctionalized and peptide-functionalized microgels should be characterized for electrophoretic mobility to determine the overall charge of the microgel. In order to determine the influence of charged groups on fibrin polymerization, a range of 5%-20% AAc-microgels, and 5-20% aminopropyl methacrylate (which are positively charged at physiological pH) should be

synthesized and their influence on fibrin-polymerization and clot structure should be characterized.

CHAPTER 5

HYBRID MICROGEL-FIBRIN CLOTS: ALTERING FIBRIN MECHANICAL PROPERTIES

5.1 Introduction

Upon vascular injury, fibrin polymerizes to form a fibrous gel that can withstand forces exerted by flowing blood and by embedded cells. They have remarkable physical properties by stiffening strongly when deformed and become increasingly resistant to further deformation [69]. Differences in clot stiffness can have significant physiological implications, in that highly rigid clots may be prone to thrombosis, while fragile clots may lead to premature lysis and re-opening of the wound [70]. Clot stiffness is thought to be strongly dependent on fibrin thickness and flexural stiffness, branchpoint density, fibrin concentration, and the presence of cross-linking agents such as Factor XIIIa [71]. However, due to strong enzymatic regulation, it is not possible to greatly increase gel rigidity starting from the natural components of fibrin clots at concentrations close to the physiological range [72]. At physiological concentrations (4.8mg/mL), fibrin hydrogels are soft and exhibit shear storage moduli on the order of 20-30Pascals [73].

The addition of protein and polymer components during the polymerization of fibrin has been shown to greatly alter fibrin network structure and clot stiffness, while maintaining adequate biological properties for physiological processes like tissue regeneration and wound healing [21, 29]. Previous studies have shown the effect of fibrin knob peptide-conjugates on clot rigidity, suggesting that the presence of GPRP-PEG conjugates generally reduces the elastic modulus of a fibrin clot [32]. Interestingly, the loss tangent, reflecting the clot viscosity was not significantly perturbed. In another study, knob ‘A’-PEG conjugates were shown to decrease the complex moduli of fibrin by 35% over controls, while knob ‘B’-PEG conjugates significantly enhance the complex

moduli [15]. These results raise questions about the role that various knob:hole interactions play in controlling the dynamics of fibrin assembly. Other attempts have been made to purposefully increase the clot rigidity of fibrin gels for tissue engineering applications. Simultaneous polymerization of polyethylene oxide (PEO) with fibrin resulted in interpenetrating networks with similar storage moduli as PEO networks alone or highly concentrated fibrin gels [21]. These hybrid gels also supported cell growth, demonstrating the feasibility of forming gels with enhanced clot rigidity but maintaining the biological function of fibrin.

We hypothesize that the polymerization of fibrin in the presence of microgels will alter the final viscoelastic properties of the gel. We examined the shear and compressive properties of hybrid fibrin-microgel gels using fibrin concentrations of 4 and 8mg/mL protein, in order to observe gels with mechanical properties high enough to be accurately measured by the instruments used. Fibrin-microgel networks are expected to have improved bulk mechanical strength at lower fibrinogen concentrations, but because the formation of the fibrin-microgel assembly is due to multiple noncovalent interactions, it is possible that these microgels add a viscous component to the gel on the order of a cell encountering the network. Further studies will need to be performed to determine the effect of microgels on cell growth, matrix remodeling, and differentiation.

5.2 Methods

5.2.1 Materials

Synthesized unfunctionalized pNIPAm microgels, GPRPFPAC-microgels, and GPSPFPAC-microgels, all described in Chapter 3, were used for these studies. The same chemicals were used as in section 4.2.1. for making assay buffers. Human fibrinogen FIB-3 and human α-thrombin were purchased from Enzyme Research Laboratories (South Bend, IN).

5.2.2 Bulk Rheology of Fibrin-Microgel Clots

A Physica MCR 501 rheometer (Anton Paar, Hertford Herts, UK) was used to examine the viscoelastic properties of fibrin clots in the presence of microgels. For the fibrin control, the reaction components, fibrinogen and thrombin, were thoroughly mixed in HEPES +Ca buffer in a 9:1 volume ratio for a final volume of 200 ul, a final fibrinogen concentration of 8 mg/mL, and a final thrombin concentration of 1 U/mL. For samples containing microgels, the microgels were added to the fibrinogen solution and allowed to incubate at least 1 hour prior to experiments for a final concentration in the total clotting mixture of 1 and 2 mg/mL. After mixing in the thrombin solution, 180 uL of the clotting mixture was quickly transferred to the center of the bottom plate of a cone-plate fixture set-up (2.014° cone angle, and 24.960 mm diameter). The cone was quickly lowered to the measurement position, and the sample was allowed to polymerize at room temperature for 2 hours before taking measurements. In order to prevent evaporation of the sample, dH_2O was applied to a ring surrounding the exposed surfaces of the clots in a humidity chamber surrounding the cone-plate set up.

Measurements were taken in oscillation mode at 0.5% constant strain over a frequency range of 0.05 and 50 Hz at 6 points/decade. The storage modulus (G'), a measure of the elastic energy stored during the deformation imposed by one oscillation of the rheometer, calculated by the Rheoplus software, was used as a measure of clot rigidity. The loss modulus (G"), the energy dissipated by the clot during deformation, was also recorded. Each condition was tested with at least 3 samples.

5.2.3 Bulk Compression of Fibrin-Microgel Clots

A Bose EnduraTEC^{TM} ELF 3200 Uniaxial Testing System (Bose Corporation ElectroForce, Eden Prairie, MN) was used to perform compression tests on 4 and 8 mg/mL fibrin clots containing 1 and 2 mg/mL microgels. Clots were polymerized with 1 U/mL thrombin in HEPES +Ca buffer for 2 hours in a silicone mold prior to taking

measurements. The silicone mold consisted of two layers of a CoverWell™ perfusion chamber gasket (Invitrogen, Frederick, Maryland), 9 mm in diameter and 2.5 mm deep, with the final dimensions of the samples being 9 mm in diameter and 5 mm in height. Strain at 10, 20, 30, 40, and 50% were applied at 1 Hz and all experiments were conducted at room temperature, with each condition being tested with at least 3 samples.

5.3 Results

5.3.1 Strength of Fibrin-Microgel Clots Under Shear

Frequency sweeps of 8 mg/mL fibrin clots polymerized in the presence of 1 mg/mL microgels at 0.5% and 0.46 Hz, showed only significant differences between the unfunctionalized microgel and control condition (Fig. 14A, B). The fibrin control and peptide-functionalized microgels exhibit similar storage moduli, however the addition of unfunctionalized microgels significantly increased the storage modulus of the bulk fibrin-microgel clot (Fig. 14A). Interestingly the loss moduli was increased for all microgel containing clots compared to the control suggesting that microgels enhance the viscous component of an overall fibrin gel (Fig. 14B). For clots polymerized in the presence of 2 mg/mL microgels, the gels exhibit generally lower storage and loss moduli than the 1 mg/mL microgel conditions (Fig. 14C, D). The storage modulus of clots polymerized in the presence of 2.5 mg/mL unfunctionalized microgels is significantly greater than all other groups (Fig. 14C). The effect of an increase in the loss modulus due to microgel incorporation is lost in the 2.5 mg/mL microgel case where peptide-functionalized microgels exhibit similar loss moduli as the control (Fig. 14D). Interestingly, GPRPFPAC-microgels and the nonbinding control GPSPFPAC-microgels do not have significant differences in storage and loss moduli at either concentration of microgel incorporation.

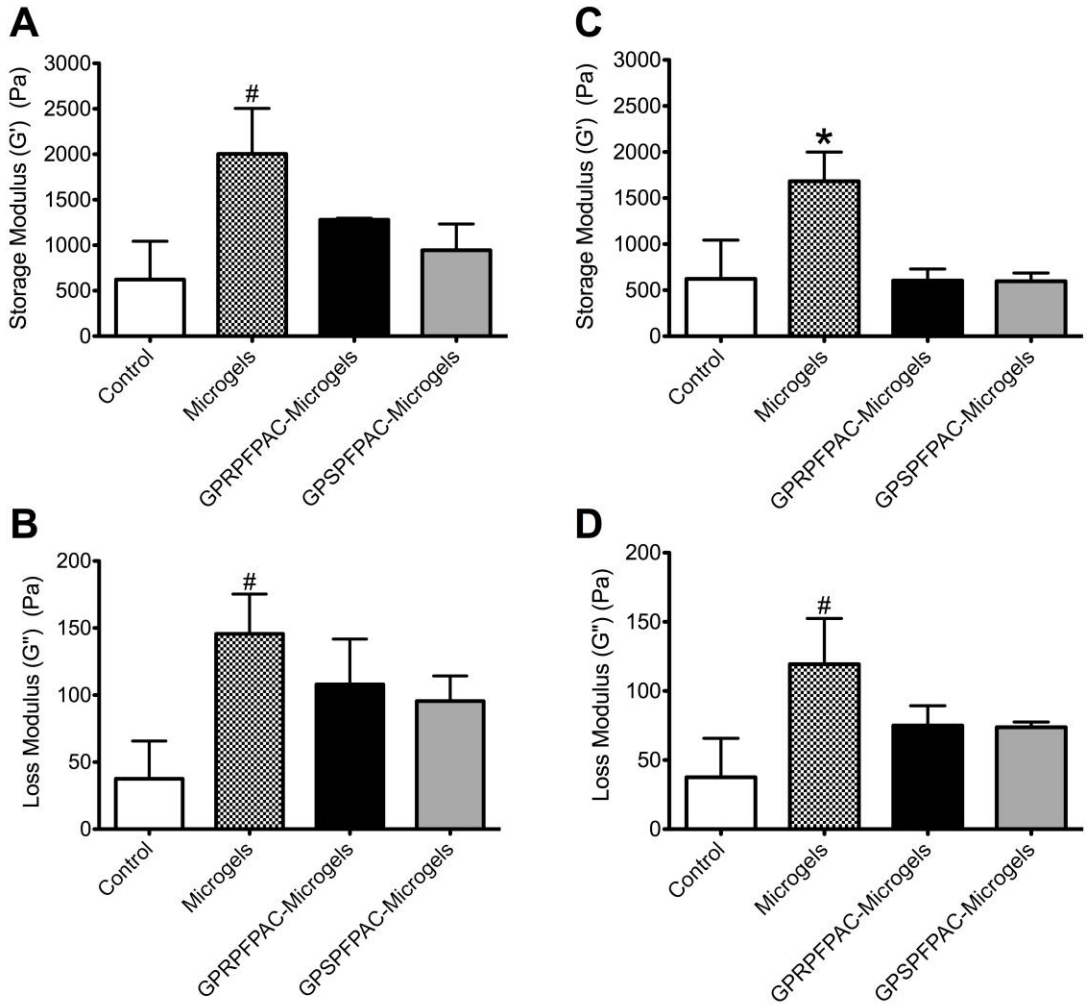

Figure 14. Rheological Measurements of Fibrin-Microgel Clots. (A,B) Storage and loss modulus of 8 mg/mL fibrin clots polymerized in the presence of 1 mg/mL microgels at 0.46 Hz and 0.5% strain (C,D) Storage and Loss Modulus of 8 mg/mL fibrin clots polymerized in the presence of 2 mg/mL microgels at 0.46 Hz and 0.5%strain.* denotes $p<0.05$ relative to all groups, and # denotes $p<0.05$ relative to the control group.

5.3.2 Strength of Fibrin-Microgel Clots Under Compression

Although the uniaxial compression of fibrin-microgel clots was measured for 4 and 8 mg/mL of fibrin, the results for 4 mg/mL microgels had higher error due to the detection limits of the instrument at low forces. Based on these results, only the data for 8 mg/mL clots is presented below to show statistically significant differences. For clots polymerized in the presence of 1 mg/mL microgels, the presence of GPRPFPAC-microgels significantly lowers the Young's modulus of the bulk clot compared to clots

polymerized with unfunctionalized microgels alone (Fig. 15A). This decrease in clot rigidity is expected and has been shown previously with GPRP-PEG conjugates [5, 15, 32]. Interestingly, at a concentration of 2.5 mg/mL microgels, unfunctionalized microgels significantly increase the Young's modulus of the bulk fibrin-microgel clot compared to all other groups (Fig. 15B). At this concentration, the compressive strength of GPRPFPAC-microgel containing clots is comparable to the control and GPSPFPAC-microgel containing clots.

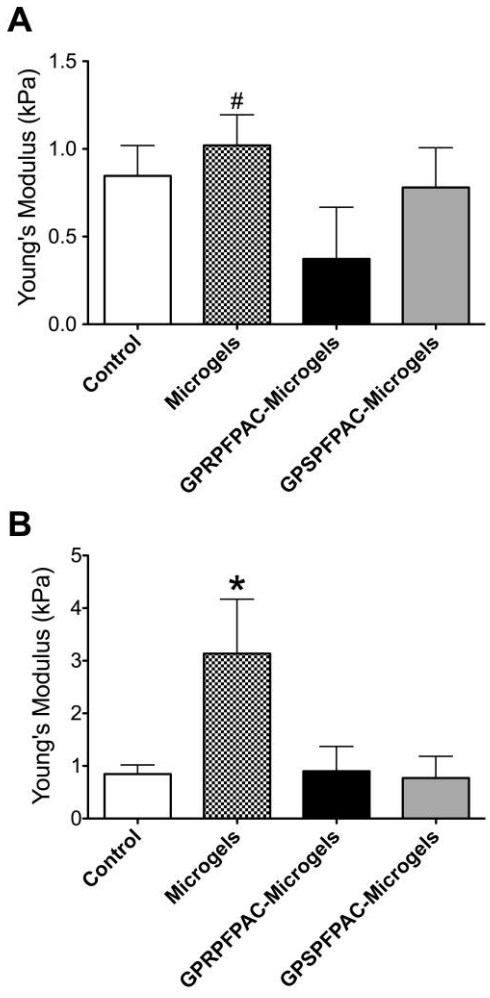

Figure 15. Uniaxial Compression Measurements of Fibrin-Microgel Clots. (A) Young's modulus of 8 mg/mL fibrin clots polymerized in the presence of 1 mg/mL microgels. (B)Young's modulus of 8 mg/mL fibrin clots polymerized in the presence of 2 mg/mL microgels. * denotes $p<0.05$ relative to all groups.

5.4 Discussion

The most notable differences in the viscoelastic properties of fibrin-microgel gels occur with unfunctionalized microgels at a concentration of 2.5 mg/mL in the final clot. The results show a significant increase in the storage and Young's modulus as compared to all other groups. It is uncertain why unfunctionalized microgels display these characteristics, but it is possible that microgel charge plays a central role in altering fibrin network structure and physical properties. Additionally, at 1 mg/mL microgel conditions, the loss moduli appear to be greater than the control clot suggesting that microgels add to the viscous component of the bulk gel. This carries potentially interesting questions for modulating the viscoelastic properties of fibrin matrices through the incorporation of microgels for determining cell fate. Native extracellular matrices are comprised of an elastic component such as collagen fibers, but are also embedded in a viscous component consisting of a variety of different glycosaminoglycans such as hyaluronic acid that promote angiogenesis. By being able to control both the bulk strength of the gel and the viscous components on the order of a cell interacting with the matrix, it might be possible to utilize these hybrid matrices for a better understanding of how cell fate is influenced by cell-matrix interactions.

CHAPTER 6

CONCLUSIONS AND FUTURE WORK

6.1 Conclusion

In this study we explored the potential of fibrin knob peptide-displaying microgels to form a colloidal assembly in the presence of fibrinogen, and observed the effect of microgel incorporation on fibrin polymerization kinetics, network structure, and final physical properties of the matrix. Chapter 3 demonstrated our ability to synthesize and functionalized ultra-low cross-linked microgels with fibrin knob peptides. The results from Chapter 4 indicate that the particular conditions that we explored for microgel concentration and peptide conjugation did not facilitate the rapid formation of a gel assembly. However, traditional tools for characterizing fibrin assembly may not be applicable to microgel-fibrinogen interactions, and other characterizing tools need to be explored to determine the dynamic interaction of active knob peptide-displaying microgels with fibrinogen.

In regards to fibrin polymerization, we were able to discern distinct trends despite stark differences in the properties of a fibrin network in the presence of unfunctionalized microgels and peptide conjugated microgels. Chapter 4 demonstrated the effect of microgels on polymerization rate, with increasing concentrations of microgels impeding fibrin network assembly and protein incorporation at low thrombin concentrations, while increasing the network's susceptibility to fibrinolysis. In Chapter 5 we explored the resulting mechanical properties of a hybrid fibrin-microgel gel, and revealed that microgels significantly alter the viscoelastic properties of a bulk gel with various effects at different concentrations.

The results from these studies introduce several questions about the interactions of microgels with fibrin(ogen), including the effect of peptide ligand density, microgel size and porosity, the effect of macromolecular crowding on fibrin assembly, and microgel charge interactions with fibrin. Exploring these effects in more detailed studies will help clarify our understanding about microgel interaction with fibrinogen and microgel interaction with a forming matrix.

6.2 Investigating Angiogenesis Properties of Hybrid Clots

In addition to understanding the influence of microgels on fibrin polymerization and structure, for viable applications as a hemostatic or tissue engineered construct, it will be necessary to probe the effect of microgel incorporation into a fibrin network on cell fate. Several parameters such as microgel concentration, microgel functionality with different peptide or protein displaying moeties, microgel charge, and the influence of the volume phase transition of the microgels in physiological conditions are expected to play a key role in determining cell fate.

Fibrin-microgel networks with heterogenous clot structure, and distinct mechanical properties present unique architectures in which to study cell growth and differentiation. As previously described in earlier discussion sections, because the microgels are not physically cross-linked into a fibrin network, the colloidal assembly of microgels within a fibrin matrix have the potential of significantly altering the viscoelasticity of fibrin networks on both the macroscopic and microscopic scale. By adding a polymer component to a fibrin gel, the general trend shows an increase in network stiffness, however at the size scale of a cell penetrating through a fibrin-microgel matrix, the noncovalent microgel assembly has the possibility of presenting a viscous component to the network thereby allowing cells to “push” through the microgel assembly and possibly enhancing the angiogenic potential of fibrin-microgel gels. These

fibrin-microgel networks may provide an interesting system to study the influence of cell-matrix interactions on cell fate.

We have established several angiogenesis models, including a microvessel construct model [15] and a HUVEC +fibroblast model that may be used to determine the angiogenesis potential of hybrid-microgel networks. Previous studies of cell growth in thermogelable pNIPAm microgel dispersions alone, showed that acrylic acid content had an adverse effect on cell culturing, at concentrations of AAc up to 5% [74]. While the presence of fibrin may alter these characteristics of a hybrid gel, the potential effects of AAc toxicity need to be taken into consideration in the next generation of peptide-microgel constructs for more optimal control of fibrin matrix properties for tissue regeneration applications.

APPENDIX A

FIBRIN POLYMERIZATION IN THE PRESENCE OF FLUORESCENTLY LABELED MICROGELS

Based on confocal images of microgel incorporated fibrin networks in Section 4.3.4, it was suspected that the areas not occupied by fibrin fibers are filled with space filling microgels. In order to visualize the interaction of microgels in a fibrin network, pNIPAm microgels were synthesized containing 0.1 M 4-acrylamidofluorescein (AFA) following the same synthesis protocol described in Section 3.2.2, but with the addition of 0.1 M AFA to the solution prior to initiation. 1 mg/mL and 2 mg/mL fibrin clots containing 0.25 mg/mL, 0.5 mg/mL and 1 mg/mL AFA-microgels were prepared similarly to the samples in Section 4.2.5 and imaged using the Zeiss 510 laser scanning confocal microscope (Carl Zeiss, Thornwood, NY). The AFA-microgels were excited using the Ar 488 laser, and the Alexa Fluor-555 labeled fibrinogen was observed using excitation by the He 543 laser under the multitracking mode. A 10 um Z-stack of 20 (0.53 um) slices under the 63X objective was captured for reconstructing the 3D fibrin-microgel network structure.

By observing the compiled 3D Z-stack images in Figure 16, it is clear to see that the microgels act as space filling colloids by occupying the regions in-between fibrin fibers. However, upon closer observation, by taking time series images of the fibrin-microgel network taken at 1 second intervals over the course of 10 seconds at a fixed focal plane, it is evident that the microgels are not physically crosslinked into the fibrin matrix, but diffuse throughout the open regions of the fibrin network (Figures 17 -22 found in separate files from thesis). At higher concentrations of microgels this diffusion is impeded by an increased number of microgel-microgel contacts. In addition to

microgel concentration dependent diffusion, at a higher protein concentration of 2 mg/mL, microgel diffusion is constrained by a denser fibrin matrix.

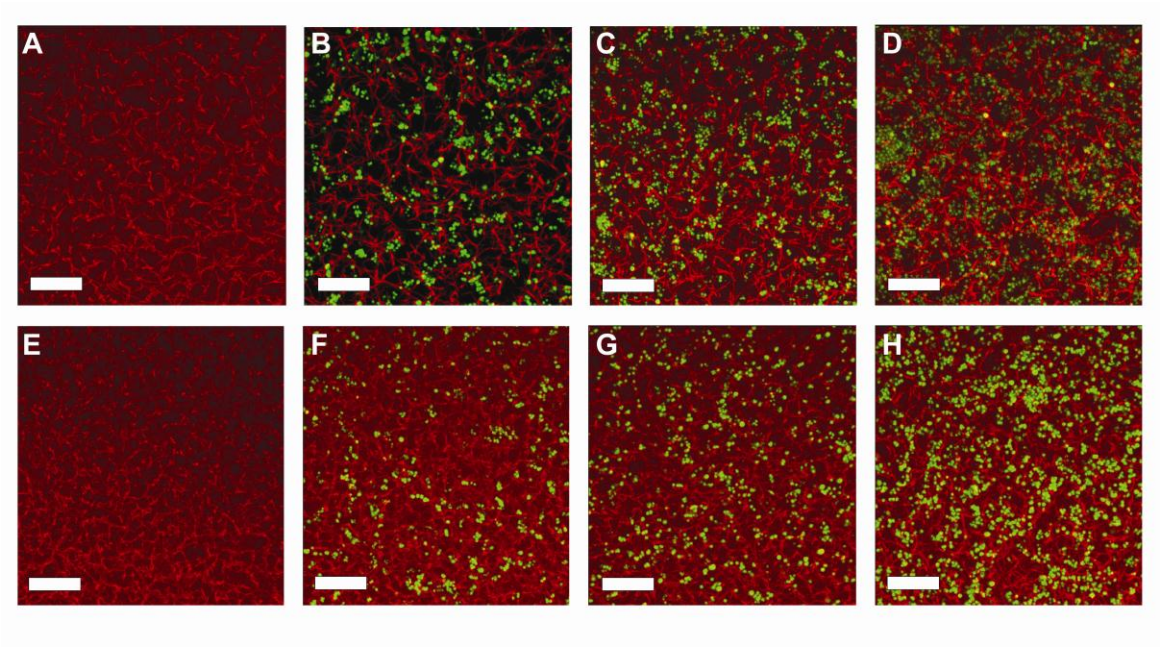

Figure 16. Confocal Z-stack Images of Fibrin Polymerized in the Presence of AFA-microgels. (A-D) 1 mg/mL fibrin. (E-H) 2 mg/mL fibrin. (A,E) fibrin controls. (B,F) 0.25 mg/mL AFA-microgels. (C,G) 0.5 mg/mL AFA-microgels (D,H) 1 mg/mL AFA-microgels. Scale bar = 20 um.

In order to determine if positive binding GPRPPFAC-microgels would be effectively crosslinked into the network by being incorporated into fibrin fibers through knob:hole interactions, GPRPFPAC peptides were conjugated to (2.5%AAc, 2.5% PEG-CH3)-AFA-microgels and polymerized into a fibrin-microgel clot. Z-stack confocal images in Figure 23 show an altered fibrin structure in the presence of GPRPFPAC-conjugated microgels compared to controls. Short and thick, highly branched structures are exhibited, similar to fibrin polymerized in the presence of nonfluorescently labeled GPRPFPAC-microgels. However, time series confocal images of a single focal plane, show that GPRPFPAC-conjugated microgels do not bind to a fibrin matrix, but also diffuse throughout the fiber network like unfunctionalized microgels (Fig. 24 found in separate file from thesis). A number of different factors might be the cause of this,

including heterogeneous ligand density that does not allow for the formation of sufficient peptide-fibrinogen interactions to stabilize the microgel within the network and noncovalent knob:hole interactions that do not permit permanent physical cross-linking of the microgel into the network.

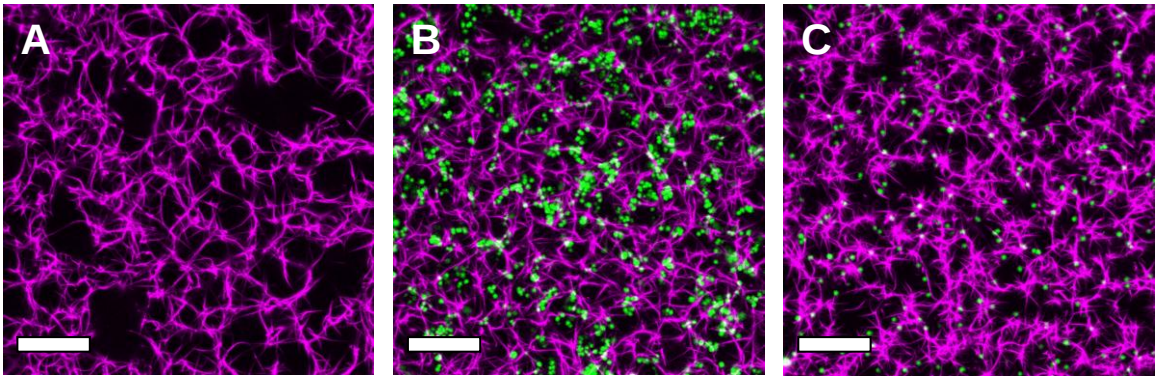

Figure 23: Confocal Z-stack images of GPRPFPAC-AFA Microgel Containing Clots. (A) 1 mg/mL fibrin control (B) 0.5 mg/mL AFA microgels (C) 0.5 mg/mL GPRPFPAC-AFA microgels. Scale bar = 20 um.

The conjugation strategy for peptide-AFA-microgels was altered slightly due to the decreased stability of fluorescently labeled microgels modified with peptides. Several approaches for peptide conjugation to various types of fluorescently labeled 5% pNIPAm ULC microgels yielded microgels that either resulted in a loss of fluorescence upon the conjugation of peptides or permanent aggregation upon lyophilization of the peptide-microgel conjugate. It is unclear why there might be a loss of fluorescence upon the conjugation of peptides to fluorescently labeled microgels. Some possibilities that have been discussed are that the peptides react with the fluorophores in a forster resonance energy transfer reaction (FRET) or that free radicals remaining within the microgel solution cause quenching upon the addition of peptides. Further investigation of the optimal conjugation conditions using ultra-low cross-linked microgels needs to be explored. As for the problems regarding lyophilization, GPRPFPAC- peptides have an overall charge of +1, which might interact with residual AAc groups on weakly stable fluorescently labeled ULC microgels. While they do not aggregate in solution, upon

lyophilization the charge interactions between peptides and AAc groups and polymer chain entanglement between microgels causes permanent aggregation. The energy required to resuspend the microgels in solution is too great to overcome the charge interactions of the peptide-AAc groups and polymer chain entangling between microgels.

In addition to problems with peptide conjugation, the use of fluorescently labeled microgels, renders them hard to characterize. The background fluorescence of AFA-microgels interferes with the CBQCA fluorescence-based peptide quantitation assay, impeding accurate peptide determination. In order to disconnect the effect of microgels on characterizing the peptide conjugated, using a peptide cleavable linker to conjugate the peptides to the microgels might be a better approach worth exploring in future studies using fluorescently labeled microgels.

REFERENCES

[1] Evans JA, van Wessem KJP, McDougall D, Lee KA, Lyons T, Balogh ZJ. Epidemiology of Traumatic Deaths: Comprehensive Population-Based Assessment. World Journal of Surgery. 2010;34:158-63.

[2] Sauaia A, Moore FA, Moore EE, Moser KS, Brennan R, Read RA, et al. EPIDEMIOLOGY OF TRAUMA DEATHS - A REASSESSMENT. Journal of Trauma-Injury Infection and Critical Care. 1995;38:185-93.

[3] Pfeifer R, Tarkin IS, Rocos B, Pape HC. Patterns of mortality and causes of death in polytrauma patients-Has anything changed? Injury-International Journal of the Care of the Injured. 2009;40:907-11.

[4] Achneck HE, Sileshi B, Jamiolkowski RM, Albala DM, Shapiro ML, Lawson JH. A Comprehensive Review of Topical Hemostatic Agents Efficacy and Recommendations for Use. Annals of Surgery. 2010;251:217-28.

[5] Stabenfeldt SE, Aboujamous NM, Soon ASC, Barker TH. A New Direction for Anticoagulants: Inhibiting Fibrin Assembly With PEGylated Fibrin Knob Mimics. Biotechnology and Bioengineering. 2011;108:2424-33.

[6] Schmoekel HG, Weber FE, Schense JC, Gratz KW, Schawalder P, Hubbell JA. Bone repair with a form of BMP-2 engineered for incorporation into fibrin cell ingrowth matrices. Biotechnology and Bioengineering. 2005;89:253-62.

[7] Lord ST. Fibrinogen and fibrin: scaffold proteins in hemostasis. Current Opinion in Hematology. 2007;14:236-41.

[8] Weisel JW. Which knobs fit into which holes in fibrin polymerization? Journal of Thrombosis and Haemostasis. 2007;5:2340-3.

[9] Ariens RAS, Lai TS, Weisel JW, Greenberg CS, Grant PJ. Role of factor XIII in fibrin clot formation and effects of genetic polymorphisms. Blood. 2002;100:743-54.

[10] Janmey PA, Winer JP, Weisel JW. Fibrin gels and their clinical and bioengineering applications. Journal of the Royal Society Interface. 2009;6:1-10.

[11] Stabenfeldt SE, Gossett JJ, Barker TH. Building better fibrin knob mimics: an investigation of synthetic fibrin knob peptide structures in solution and their dynamic binding with fibrinogen/fibrin holes. Blood. 2010;116:1352-9.

[12] Meng Z, Cho JK, Breedveld V, Lyon LA. Physical Aging and Phase Behavior of Multiresponsive Microgel Colloidal Dispersions. Journal of Physical Chemistry B. 2009;113:4590-9.

[13] Meng ZY, Cho JK, Debord S, Breedveld V, Lyon LA. Crystallization behavior of soft, attractive microgels. Journal of Physical Chemistry B. 2007;111:6992-7.

[14] Ahmed TAE, Dare EV, Hincke M. Fibrin: A versatile scaffold for tissue engineering applications. Tissue Engineering Part B-Reviews. 2008;14:199-215.

[15] Stabenfeldt SE, Gourley M, Krishnan L, Hoying JB, Barker TH. Engineering fibrin polymers through engagement of alternative polymerization mechanisms. Biomaterials. 2012;33:535-44.

[16] Laurens N, Koolwijk P, De Maat MPM. Fibrin structure and wound healing. Journal of Thrombosis and Haemostasis. 2006;4:932-9.

[17] Mosesson MW. Fibrinogen and fibrin structure and functions. Journal of Thrombosis and Haemostasis. 2005;3:1894-904.

[18] Jockenhoevel S, Zund G, Hoerstrup SP, Chalabi K, Sachweh JS, Demircan L, et al. Fibrin gel-advantages of a new scaffold in cardiovascular tissue engineering. European Journal of Cardio-Thoracic Surgery. 2001;19:424-30.

[19] Mol A, van Lieshout MI, Veen CGD, Neuenschwander S, Hoerstrup SP, Baaijens FPT, et al. Fibrin as a cell carrier in cardiovascular tissue engineering applications. Biomaterials. 2005;26:3113-21.

[20] Lee CR, Grad S, Gorna K, Gogolewski S, Goessl A, Alini M. Fibrin-polyurethane composites for articular cartilage tissue engineering: A preliminary analysis. Tissue Engineering. 2005;11:1562-73.

[21] Akpalo E, Bidault L, Boissiere M, Vancaeyzeele C, Fichet O, Larreta-Garde V. Fibrin-polyethylene oxide interpenetrating polymer networks: New self-supported biomaterials combining the properties of both protein gel and synthetic polymer. Acta Biomaterialia. 2011;7:2418-27.

[22] Van Lieshout M, Peters G, Rutten M, Baaijens F. A knitted, fibrin-covered polycaprolactone scaffold for tissue engineering of the aortic valve. Tissue Engineering. 2006;12:481-7.

[23] Collen A, Smorenburg SM, Peters E, Lupu F, Koolwijk P, Van Noorden C, et al. Unfractionated and low molecular weight heparin affect fibrin structure and angiogenesis in vitro. Cancer Research. 2000;60:6196-200.

[24] Rao RR, Peterson AW, Ceccarelli J, Putnam AJ, Stegemann JP. Matrix composition regulates three-dimensional network formation by endothelial cells and mesenchymal stem cells in collagen/fibrin materials. Angiogenesis. 2012;15:253-64.

[25] Jha AK, Malik MS, Farach-Carson MC, Duncan RL, Jia X. Hierarchically structured, hyaluronic acid-based hydrogel matrices via the covalent integration of microgels into macroscopic networks. Soft Matter. 2010;6:5045-55.

[26] Lesman A, Koffler J, Atlas R, Blinder YJ, Kam Z, Levenberg S. Engineering vessel-like networks within multicellular fibrin-based constructs. Biomaterials. 2011;32:7856-69.

[27] Peled E, Boss J, Bejar J, Zinman C, Seliktar D. A novel poly(ethylene glycol)-fibrinogen hydrogel for tibial segmental defect repair in a rat model. Journal of Biomedical Materials Research Part A. 2007;80A:874-84.

[28] Seliktar D. Extracellular stimulation in tissue engineering. In: Sideman S, Beyar R, Landesberg A, editors. Communicative Cardiac Cell2005. p. 386-94.

[29] Almany L, Seliktar D. Biosynthetic hydrogel scaffolds made from fibrinogen and polyethylene glycol for 3D cell cultures. Biomaterials. 2005;26:2467-77.

[30] Dikovsky D, Bianco-Peled H, Seliktar D. The effect of structural alterations of PEG-fibrinogen hydrogel scaffolds on 3-D cellular morphology and cellular migration. Biomaterials. 2006;27:1496-506.

[31] Jing P, Rudra JS, Herr AB, Collier JH. Self-assembling peptide-polymer hydrogels designed from the coiled coil region of fibrin. Biomacromolecules. 2008;9:2438-46.

[32] Soon ASC, Lee CS, Barker TH. Modulation of fibrin matrix properties via knob:hole affinity interactions using peptide-PEG conjugates. Biomaterials. 2011;32:4406-14.

[33] Dare EV, Griffith M, Poitras P, Kaupp JA, Waldman SD, Carlsson DJ, et al. Genipin Cross-Linked Fibrin Hydrogels for in vitro Human Articular Cartilage Tissue-Engineered Regeneration. Cells Tissues Organs. 2009;190:313-25.

[34] Laudano AP, Doolittle RF. STUDIES ON SYNTHETIC PEPTIDES THAT BIND TO FIBRINOGEN AND PREVENT FIBRIN POLYMERIZATION - STRUCTURAL REQUIREMENTS, NUMBER OF BINDING-SITES, AND SPECIES-DIFFERENCES. Biochemistry. 1980;19:1013-9.

[35] Laudano AP, Doolittle RF. SYNTHETIC PEPTIDE DERIVATIVES THAT BIND TO FIBRINOGEN AND PREVENT POLYMERIZATION OF FIBRIN MONOMERS. Proceedings of the National Academy of Sciences of the United States of America. 1978;75:3085-9.

[36] Laudano AP, Doolittle RF. INFLUENCE OF CALCIUM-ION ON THE BINDING OF FIBRIN AMINO TERMINAL PEPTIDES TO FIBRINOGEN. Science. 1981;212:457-9.

[37] Soon ASC, Stabenfeldt SE, Brown WE, Barker TH. Engineering fibrin matrices: The engagement of polymerization pockets through fibrin knob technology for the delivery and retention of therapeutic proteins. Biomaterials. 2010;31:1944-54.

[38] Gehrke SH. SYNTHESIS, EQUILIBRIUM SWELLING, KINETICS, PERMEABILITY AND APPLICATIONS OF ENVIRONMENTALLY RESPONSIVE GELS. Advances in Polymer Science. 1993;110:81-144.

[39] Hoffman AS. Hydrogels for biomedical applications. Advanced Drug Delivery Reviews. 2002;54:3-12.

[40] Yeomans K. Hydrogels-very versatile materials. Chem Rev. 2002;10:2-5.

[41] Nayak S, Lyon LA. Soft nanotechnology with soft nanoparticles. Angewandte Chemie-International Edition. 2005;44:7686-708.

[42] Schild HG. POLY (N-ISOPROPYLACRYLAMIDE) - EXPERIMENT, THEORY AND APPLICATION. Progress in Polymer Science. 1992;17:163-249.

[43] Saunders BR, Vincent B. Microgel particles as model colloids: theory, properties and applications. Advances in Colloid and Interface Science. 1999;80:1-25.

[44] Pelton R. Temperature-sensitive aqueous microgels. Advances in Colloid and Interface Science. 2000;85:1-33.

[45] Jones CD, Lyon LA. Synthesis and characterization of multiresponsive core-shell microgels. Macromolecules. 2000;33:8301-6.

[46] Gan DJ, Lyon LA. Interfacial nonradiative energy transfer in responsive core-shell hydrogel nanoparticles. Journal of the American Chemical Society. 2001;123:8203-9.

[47] Gao J, Frisken BJ. Cross-linker-free N-isopropylacrylamide gel nanospheres. Langmuir. 2003;19:5212-6.

[48] Gao J, Frisken BJ. Influence of reaction conditions on the synthesis of self-cross-linked N-isopropylacrylamide microgels. Langmuir. 2003;19:5217-22.

[49] Blackburn WH, Dickerson EB, Smith MH, McDonald JF, Lyon LA. Peptide-Functionalized Nanogels for Targeted siRNA Delivery. Bioconjugate Chemistry. 2009;20:960-8.

[50] Kawaguchi H, Kisara K, Takahashi T, Achiha K, Yasui M, Fujimoto K. Versatility of thermosensitive particles. Macromolecular Symposia. 2000;151:591-8.

[51] Delair T, Meunier F, Elaissari A, Charles MH, Pichot C. Amino-containing cationic latex-oligodeoxyribonucleotide conjugates: application to diagnostic test sensitivity

enhancement. Colloids and Surfaces a-Physicochemical and Engineering Aspects. 1999;153:341-53.

[52] Riener CK, Kada G, Gruber HJ. Quick measurement of protein sulfhydryls with Ellman's reagent and with 4,4'-dithiodipyridine. Analytical and Bioanalytical Chemistry. 2002;373:266-76.

[53] Graves SW, Woods TA, Kim H, Nolan JP. Direct fluorescent staining and analysis of proteins on microspheres using CBQCA. Cytometry Part A. 2005;65A:50-8.

[54] Blomback B, Hessel B, Hogg D, Therkildsen L. 2-STEP FIBRINOGEN-FIBRIN TRANSITION IN BLOOD-COAGULATION. Nature. 1978;275:501-5.

[55] Carr ME, Gabriel DA, McDonagh J. INFLUENCE OF FACTOR-XIII AND FIBRONECTIN ON FIBER SIZE AND DENSITY IN THROMBIN-INDUCED FIBRIN GELS. Journal of Laboratory and Clinical Medicine. 1987;110:747-52.

[56] Carr ME, Kaminski M, McDonagh J, Gabriel DA. INFLUENCE OF IONIC-STRENGTH, PEPTIDE RELEASE AND CALCIUM ON THE STRUCTURE OF REPTILASE AND THROMBIN DERIVED FIBRIN GELS. Thrombosis and Haemostasis. 1985;54:159-.

[57] Di Stasio E, Nagaswami C, Weisel JW, Di Cera E. Cl- regulates the structure of the fibrin clot. Biophysical Journal. 1998;75:1973-9.

[58] Weisel JW, Nagaswami C. COMPUTER MODELING OF FIBRIN POLYMERIZATION KINETICS CORRELATED WITH ELECTRON-MICROSCOPE AND TURBIDITY OBSERVATIONS - CLOT STRUCTURE AND ASSEMBLY ARE KINETICALLY CONTROLLED. Biophysical Journal. 1992;63:111-28.

[59] Kolev K, Tenekedjiev K, Komorowicz E, Machovich R. Functional evaluation of the structural features of proteases and their substrate in fibrin surface degradation. Journal of Biological Chemistry. 1997;272:13666-75.

[60] Veklich Y, Francis CW, White J, Weisel JW. Structural studies of fibrinolysis by electron microscopy. Blood. 1998;92:4721-9.

[61] Sakharov DV, Nagelkerke JF, Rijken DC. Rearrangements of the fibrin network and spatial distribution of fibrinolytic components during plasma clot lysis - Study with confocal microscopy. Journal of Biological Chemistry. 1996;271:2133-8.

[62] Collet JP, Lesty C, Montalescot G, Weisel JW. Dynamic changes of fibrin architecture during fibrin formation and intrinsic fibrinolysis of fibrin-rich clots. Journal of Biological Chemistry. 2003;278:21331-5.

[63] Minton AP. The influence of macromolecular crowding and macromolecular confinement on biochemical reactions in physiological media. Journal of Biological Chemistry. 2001;276:10577-80.

[64] Chen C, Loe F, Blocki A, Peng Y, Raghunath M. Applying macromolecular crowding to enhance extracellular matrix deposition and its remodeling in vitro for tissue engineering and cell-based therapies. Advanced Drug Delivery Reviews. 2011;63:277-90.

[65] Chebotareva NA, Kurganov BI, Livanova NB. Biochemical effects of molecular crowding. Biochemistry-Moscow. 2004;69:1239-+.

[66] Ellis RJ. Macromolecular crowding: obvious but underappreciated. Trends in Biochemical Sciences. 2001;26:597-604.

[67] Lareu RR, Arsianti I, Subramhanya HK, Peng Y, Raghunath M. In vitro enhancement of collagen matrix formation and crosslinking for applications in tissue engineering: A preliminary study. Tissue Engineering. 2007;13:385-91.

[68] Hojima Y, Behta B, Romanic AM, Prockop DJ. CLEAVAGE OF TYPE-I PROCOLLAGEN BY C-PROTEINASES AND N-PROTEINASES IS MORE RAPID IF THE SUBSTRATE IS AGGREGATED WITH DEXTRAN SULFATE OR POLYETHYLENE-GLYCOL. Analytical Biochemistry. 1994;223:173-80.

[69] Piechocka IK, Bacabac RG, Potters M, MacKintosh FC, Koenderink GH. Structural Hierarchy Governs Fibrin Gel Mechanics. Biophysical Journal. 2010;98:2281-9.

[70] Standeven KF, Ariens RAS, Grant PJ. The molecular physiology and pathology of fibrin structure/function. Blood Reviews. 2005;19:275-88.

[71] Ryan EA, Mockros LF, Weisel JW, Lorand L. Structural origins of fibrin clot rheology. Biophysical Journal. 1999;77:2813-26.

[72] Akpalo E, Larreta-Garde V. Increase of fibrin gel elasticity by enzymes: A kinetic approach. Acta Biomaterialia. 2010;6:396-402.

[73] Collet JP, Shuman H, Ledger RE, Lee ST, Weisel JW. The elasticity of an individual fibrin fiber in a clot. Proceedings of the National Academy of Sciences of the United States of America. 2005;102:9133-7.

[74] Gan TT, Guan Y, Zhang YJ. Thermogelable PNIPAM microgel dispersion as 3D cell scaffold: effect of syneresis. Journal of Materials Chemistry. 2010;20:5937-44.